EFFECT OF ORGANOCLAY REINFORCEMENT ON PYROLYTIC-LIGNIN-BASED CARBON FIBRES

by

Wei Qin

B. Eng., Donghua University, 2007

A THESIS SUBMITTED IN PARTIAL FULFILLMENT OF THE REQUIREMENTS FOR THE DEGREE OF

MASTER OF SCIENCE

in

The Faculty of Graduate Studies

(Forestry)

THE UNIVERSITY OF BRITISH COLUMBIA

(Vancouver)

December 2010

Abstract

Pyrolytic lignin has negative effect on the quality of bio-oil in the application as fuel and energy source. On the other hand, pyrolytic lignin is also a potential alternative precursor for the manufacturing of general performance grade carbon fibre. Since clay or layered silicate reinforcement has been demonstrated to enhance the mechanical properties of many polymers, improvement of mechanical properties of carbon fibre fabricated in this work is expected. This thesis focuses on the proof-of-concept study of pyrolytic-lignin-based carbon fibres and investigates the potential of organoclay reinforcement in improving the mechanical properties of the resultant carbon fibres.

In the process of carbon fibre preparation, the pretreatment (thermal treatment under reduced pressure) was found to be a critical step in the successful preparation of carbon fibres from pyrolytic lignin. Without pretreatment, the pyrolytic lignin tended to develop hollow structures during spinning and the spun fibres fuse when thermostabilized. In the pretreatment, higher temperatures and longer time (170-180^{o}C and 4-6 hrs) led to poor fibre spinning of pyrolytic lignin, whereas lower temperature and shorter time (150^{o}C and 0.5-2 hrs) resulted in lignin fibres fusing in the thermostabilization process. Only a narrow window between these two extremes is suitable for carbon fibre production. By choosing the treatment condition (160°C, 30KPa for 1h) that gives the best fibre spinning, pyrolytic-lignin-based carbon fibres were fabricated, with mechanical properties and yield comparable to those based on technical lignins.

Two organoclays were employed containing modifiers with different hydrophobicity. The tensile strength of carbon fibres were improved by 12% to ~440 MPa at a 1 wt% organoclay Cloisite 30B loading. Increasing the organoclay content above 1 wt% resulted in a drop in tensile strength. The Young's modulus of pyrolytic-lignin-based carbon fibres dropped slightly upon addition of both types of organoclays (~32 GPa) and decreased as organoclay content increases. The addition of organoclay only slightly increased the overall yield of carbon fibre production from 45 wt% to 46-47%, which was independent of organoclay type and loading.

Table of Contents

List of Tables

List of Figures

List of Abbreviations

ANOVA: analysis of variance

DMF: dimethylformamide

DMSO: dimethyl sulfoxide

DSC: differential scanning calorimetry

GPC: gel permeation chromatography

Mn: number average molecular weight

Mw: weight average molecular weight

NMR: nuclear magnetic resonance

PAN: polyacrylonitrile

PVA: polyvinyl alcohol

PDI: polydispercity index

SEM: scanning electron microscopy

Td: decomposition temperature

Tg: glass transition temperature

THF: tetrahydrofuran

TGA: thermogravimetric analysis

Acknowledgements

I would like to acknowledge my professors, friends and colleagues at the University of British Columbia (UBC), who have made this a memorable journey.

First, I acknowledge Dr. John F. Kadla, whose support and encouragement have helped me through this process.

I would like to thank Drs. Frank Ko and Naoko Ellis for their advice and guidance.

I acknowledge Mr. Thomas Bouchard at Dynamotive Energy Systems Corporation for providing me with the illustration of fast pyrolysis process.

I thank National Research Council Canada (NRC), National Sciences and Engineering Council of Canada (NSERC) and BIOCAP Canada Foundation for founding this project and Dynamotive Energy Systems Corporation for providing the bio-oil.

Let me also say 'thank you' to all my friends and fellow lab-mates in UBC for their friendship and advice, in particular: Drs. Jennifer Braun, Yong-Sik Kim, Batia Bar-Nir, Mr. Ian Dallmeyer, Reza Korehei, Ms. Carmen Hsieh Ana Filipa Xavier and Aries Chang.

Finally, a special ‘thanks’ goes to my parents for their unconditional love and continuous support throughout my education.

1 INTRODUCTION

1.1 Lignin

Lignin is one of the most abundant biopolymers in nature. Found in all vascular plants, lignin, or "native lignin" as it is commonly referred to, provides structural support, protection from biological attack and facilitates water conduction. Due to its structural complexity and the fact that it cannot be isolated from plant tissue without introducing structural changes, it is not possible to define the exact chemical and molecular structure (Zakzeski et al., 2010). However, among the various isolated lignins, milled wood lignin (MWL) is considered to most closely represent the structure of lignin in the native state (Marchessault et al., 1982).

1.1.1 Native lignin

Native lignin is generally defined as a polyphenolic heteropolymer deriving from enzymatic dehydrogenative polymerization of three major phenylpropanoid monomers (Higuchi, 1985; Sederoff and Chang, 1991; Boerjan et al., 2003; Lebo et al., 2007), i.e., p-coumaryl alcohol, coniferyl alcohol, and sinapyl alcohol, which differ only in their degree of methoxylation on the aromatic ring (**Figure 1.1**). As the basic building blocks of lignin, they are commonly known as monolignols. For a comprehensive review of lignin biosynthesis, refer to the literature (Higuchi, 1985; Sederoff and Chang, 1991; Boerjan et al., 2003) and the references sited therein.

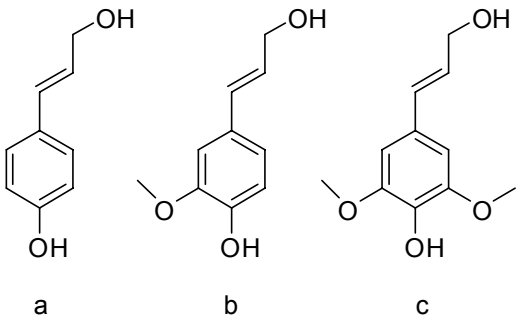

Figure 1.1 Chemical structures of the three monolignols. (a) p-coumaryl alcohol; (b) coniferyl alcohol; (c) sinapyl alcohol

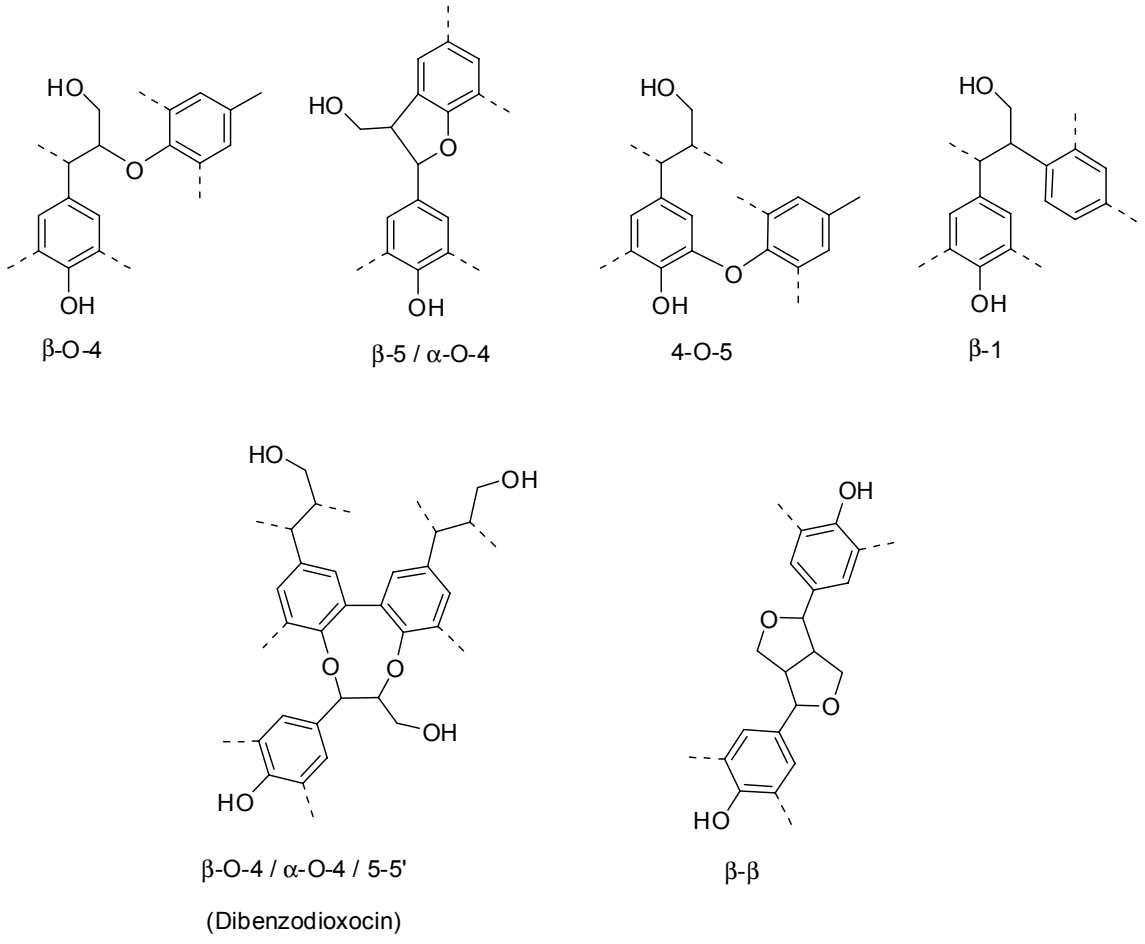

Figure 1.2 Structures of prominent interunit linkages found in native lignin (Adler, 1977)

These monolignols are generally believed to polymerize through random phenoxy radical-radical coupling reactions (Ralph et al., 2004) which result in a complex 3-dimensional cross-linked structure. The complex nature of the interunit linkages found in lignins is based on the 4 main mesomeric structures of the phenoxy radicals produced by peroxide catalyzed oxidation of the aforementioned monolignols. Coupling of these radicals gives rise to dimeric structures with different interunit linkages. The resulting dimers may be further dehydrogenated and couple with another monomeric radical. As the process of dehydrogenation and radical coupling continues, a complex 3-dimensional polymer structure develops. Of the 16 possible interunit linkages formed by such radicals, the most prominent are shown in **Figure 1.2**. **Table 1.1** lists the relative frequencies of the most prominent interunit limnkages found in a typical softwood (Spruce - *Picea abies*) (Capanema et al., 2004) and hardwood (*Eucalyptus grandis*) (Capanema et al., 2005).

Table 1.1 Frequencies of major interunit linkages in spruce (*Picea abies*) (Capanema et al., 2004) and eucalyptus (*Eucalyptus grandis*) (Capanema et al., 2005) lignin

	Interunit linkage per 100 C_9-units						
Lignin	**β-O-4[a]**	**β–β**	**β-5**	**β–1**	**4-O-5**	**5-5[a]**	**α-O-4[a]**
Spruce	45	2	9	1	4	12	16
Eucalyptus	61	3	3	2	9	3	NR[b]

[a]: includes those from Dibenzodioxocin moieties; [b]: not reported

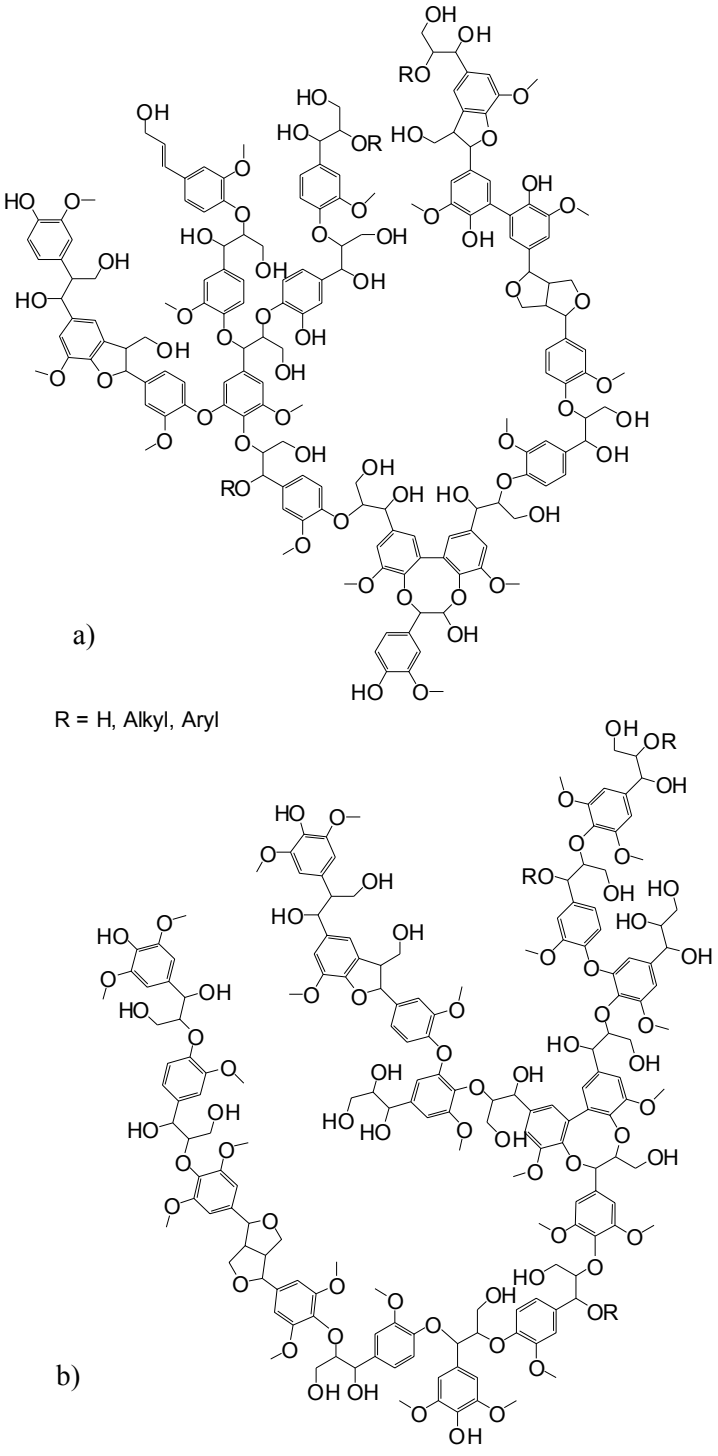

Figure 1.3 Schematic presentation of a) softwood and b) hardwood lignin structure (Kubo and Kadla, 2006)

In addition to the difference in interunit linkages, hardwood and softwood lignins also differ in the amount of functional groups present. Hardwoods typically have slightly lower phenolic hydroxyl group content (10-20/100 C_9) as compared to softwood lignin (15-30/100 C_9), but a substantially higher methoxyl content, 139-158/100 C_9 (hardwood) vs ~95/100 C_9 for softwood lignin (Adler, 1977). **Figure 1.3** gives a model structure of native lignin found in softwood and hardwood.

For over half a century considerable work has been devoted to elucidate the complex structure of lignin, and as a result a wealth of information on the structure of lignin has been obtained (Chang et al., 1975; Adler, 1977; Ralph et al., 1999; Ralph et al., 2001; Holtman et al., 2003; Capanema et al., 2004; Ralph et al., 2004; Holtman et al., 2007).

1.1.2 Industrial lignins

Commercial lignins are currently available through the chemical pulping industry, they are extracted from wood as well as some annual plants, such as straw, bagasse and flax (Smook, 1992). During the harsh conditions of chemical pulping, native lignin molecules undergo severe degradation and are chemically modified to a greater or lesser extent depending on the specific chemical pulping process (Kadla and Dai, 2006). Lignin extracted in these processes remains in the spent liquor. Majority of the lignin are not isolated but burned in chemical recovery boilers to provide energy for the system and recover process chemicals (Smook, 1992). As a result, only a small amount of lignin is

recovered and purified, having a market in many different industries for a variety of applications (Gargulak and Lebo, 2000).

Commercial lignins can be broadly classified into two classes; sulfur-containing lignin and sulfur-free lignin. Most of the commercially available lignins fall into the first category, in which lignosulfonate and Kraft lignin are of most importance. Kraft pulping is currently the dominant process in the pulping industry. This process employs a combination of sodium hydroxide and sodium sulfide to extract lignin from wood. During the delignification process, lignin is cleaved at some of its aryl-ether (β-O-4) linkages and thiol groups are introduced into the partially depolymerized lignin (Kadla and Dai, 2006). Kraft lignin (also known as sulfate lignin or alkali lignin) is obtained after isolation from the spent liquor. Analysis of the structure and functional groups present in the residual lignin show an increase in phenolic hydroxyl groups, decreased aliphatic hydroxyl content, presence of catechol and stilbene type structures, decreased coumaran (β-5), resinol (β–β), benzyl alcohol and benzyl ethers as well as an increase in carboxylic acid content (Marton, 1971; Kringstad and Morck, 1983). They have number average molecular weight in the range of 2000–3000 and a polydispersity (Mw/Mn) of 2-3 (Lebo et al., 2004).

Lignosulfonate, also known as sulfite lignin, is derived from the sulfite pulping process in which lignin is fragmented and rendered soluble in water by introducing sulfonic acid groups into its aliphatic backbone. In the presence of suitable counter-ions (Na^+, Ca^{2+}, Mg^{2+}, NH_4^+, etc.), it is soluble in water over essentially the entire useful pH range, but insoluble in most common organic solvents. Depending on the pH conditions

used the resulting lignin can vary greatly in chemical structure and macromolecular properties. Alkaline sulphite lignins closely resemble those of Kraft lignin, wherein the predominant mechanism of delignification is reaction of the sulphite nucleophiles with the quinonemethide intermediate lignin structures and preferential cleavage of the predominant β-O-4 interunit linkages (Kadla and Dai, 2006). However, under acidic conditions (acid sulphite process) sulfonation occurs involving reactions with only a few of the original lignin-lignin bonds, thereby minimizing the extent of secondary bond forming reactions. As a consequence lignosulfonates more closely represent the macromolecular structure of the native lignin (Sarkanen and Ludwig, 1971). Lignosulfonates are substantially higher in molecular weight, typically ranging from 10,000 to 40,000, and even over 100,000 for isolated high molecular weight fractions (Sarkanen and Ludwig, 1971), exhibit surface activity and are widely employed as surfactants both in pristine and modified forms (Gargulak and Lebo, 2000).

As with sulfur-containing lignins, sulfur-free lignins generally do not closely resemble the structure of native lignin. Depending on the process various changes in chemical structure and functional groups occur (Sarkanen and Ludwig, 1971). However, for certain feedstocks or potential lignin applications sulfur-free processing can have some advantages. For example, in the processing of nonwood species such as wheat straw, hemp and flax, which are much easier to delignify, Kraft pulping is not required. Alkali pulping in the absence of sodium sulphide, i.e. soda pulping sufficiently delignifies the biomass and does not require the costly, elaborate chemical recovery process associated with the Kraft process. However, the absence of the efficient

nucleophile (sodium sulphide) leads to extensive condensation reactions within the dissolved lignin (Kadla and Dai, 2006), thereby affecting its utility in various applications. As with Kraft lignin, soda lignin usually has a moderate molecular weight in the range of 1000-3000 (Gosselink et al., 2004).

More recently organic solvent-based pulping processes have again generated great interest, particularly in the concept of biofuels and the bio-refinery process (Lora and Glasser, 2002). In these processes lignin is extracted from lignocellulosic feedstocks with organic solvents or their aqueous solutions (Zhao et al., 2009). Depending on the solvent and catalyst a relatively pure stream of lignin can be obtained, however varying degrees of chemical modification are obtained depending on the process (Kubo and Kadla, 2004). Organosolv lignin usually has a relatively low molecular weight ~ 1000 with relatively broad molecular weight distributions (with polydispersity between 2 - 6) (Glasser et al., 1983).

1.1.3 Bio-refinery, fast pyrolysis and pyrolytic lignin

The development of a sustainable economy is a challenging task for human society in the 21st century. The current world economy is primarily based on non-renewable fossil fuels. However, sustainable development requires low-cost and renewable resources as feedstock for industrial production of energy, fuel and chemicals. Since biomass is relatively inexpensive and renewable, it is a potential substitute for depleting fossil resources. Thus one promising solution to this resource problem is the stepwise transition from a traditional mineral-based economy to a bio-based economy which is

built on the bio-refinery system. Similar to the traditional refinery system based on fossil fuel deriving from biomass that lived hundreds of millions of years ago, in the bio-refinery system, energy, fuel and chemicals (**Figure 1.4**) can be directly converted from today's biomass instead of fossil materials.

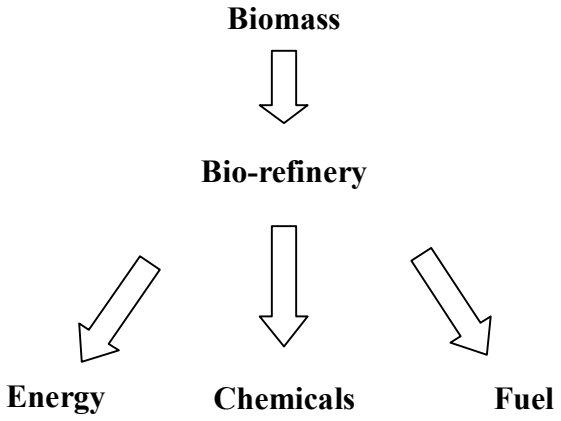

Figure 1.4 Schematic structure of the bio-refinery concept

One way to implement the bio-refinery concept is the fast pyrolysis of biomass (Brown, 2006). This process typically generates three products: syngas, bio-oil and solid char, all of which are potential sources of energy, fuel and chemicals. **Figure 1.5** illustrates the (Dynamotive) fast pyrolysis process. This is a zero-waste process, wherein the bio-oil and char have commercial applications and the syngas can be used to supply up to 75% of internal energy demands. The bio-oil can be used directly as fuel in industrial burners and boilers to provide heat and energy (Dynamotive) or alternatively combined with biodiesel (Jiang and Ellis, 2010). Bio-oil can be used to extract levoglucosan (Bennett et al., 2009) from which ethanol is produced after hydrolysis and / or fermentation. However, bio-oil suffers from instability caused by numerous self-

reactions taking place during storage, and is an area of current research (Oasmaa and Kuoppala, 2003).

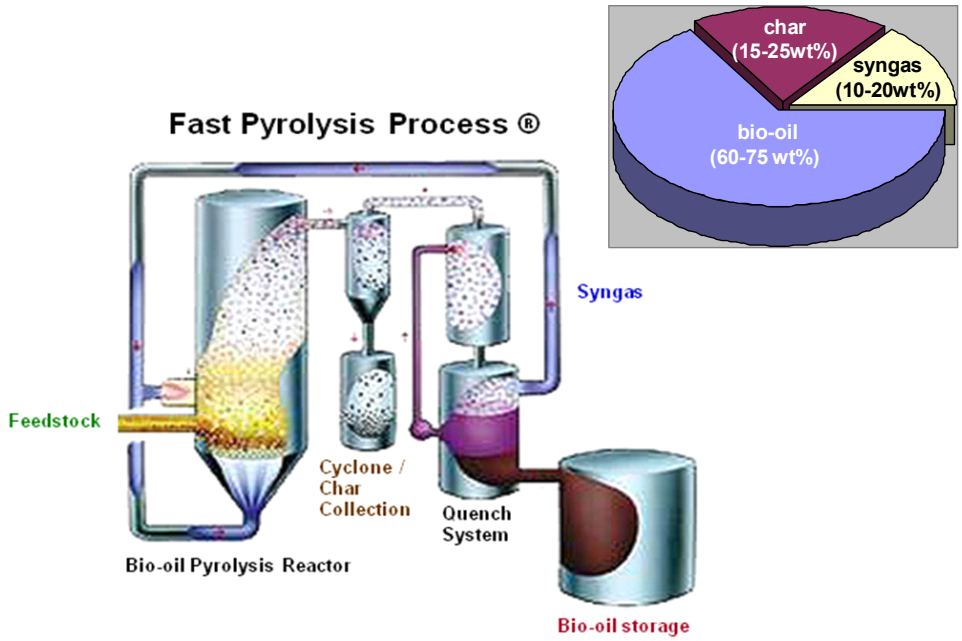

Figure 1.5 Schematic representation of a Bio-oil Pyrolysis Reactor and process product distributions (Dynamotive)

Table 1.2 lists the relative composition of bio-oil components (Walker, 2007). A large component of bio-oil is the water insoluble fraction, commonly referred to as pyrolytic lignin. At approximately 25-30% by weight, pyrolytic lignin is believed to have a negative effect on the stability of bio-oil (Bayerbach and Meier, 2009), as well as reduces the combustion efficiency of bio-oil; the complete combustion of pyrolytic lignin takes longer than that of the other components within the bio-oil. Thus, it is desirable to remove pyrolytic lignin in the upgrading process for bio-oil. However, this separation process can generate a large volume of pyrolytic lignin, which will introduce additional

costs for handling/disposal. Therefore, in order to lower the cost of this process, it is necessary to find value-adding applications for pyrolytic lignin.

Table 1.2 Bio-oil components from the fast pyrolysis of biomass (Walker, 2007)

Bio-oil Components	Concentration (wt%)
Water	20-25
Water Insoluble (Pyrolytic Lignin)	25-30
Organic Acids	5-12
Non-polar Hydrocarbons	5-10
Anhydrosugars	5-10
Other Oxygenated Compounds	10-25

The chemical and macromolecular characteristics of pyrolytic lignin are crucial for the development of value-adding applications and the requisite processing technologies. However, there are only a few studies in the literature reporting the chemical structure and characteristics of pyrolytic lignin (Scholze et al., 2001; Scholze and Meier, 2001; Bayerbach et al., 2006; Fratini et al., 2006; Bayerbach and Meier, 2009). Moreover, those reported depend strongly on the origin of biomass, the processing conditions used to produce the bio-oils (e.g. reactor type, pyrolysis temperature, etc) as well as the storage conditions and time. Although discrepancies may exist between different studies, it is

generally accepted that pyrolytic lignin consists of highly degraded lignin oligomers with relatively low molecular weights of around 1000.

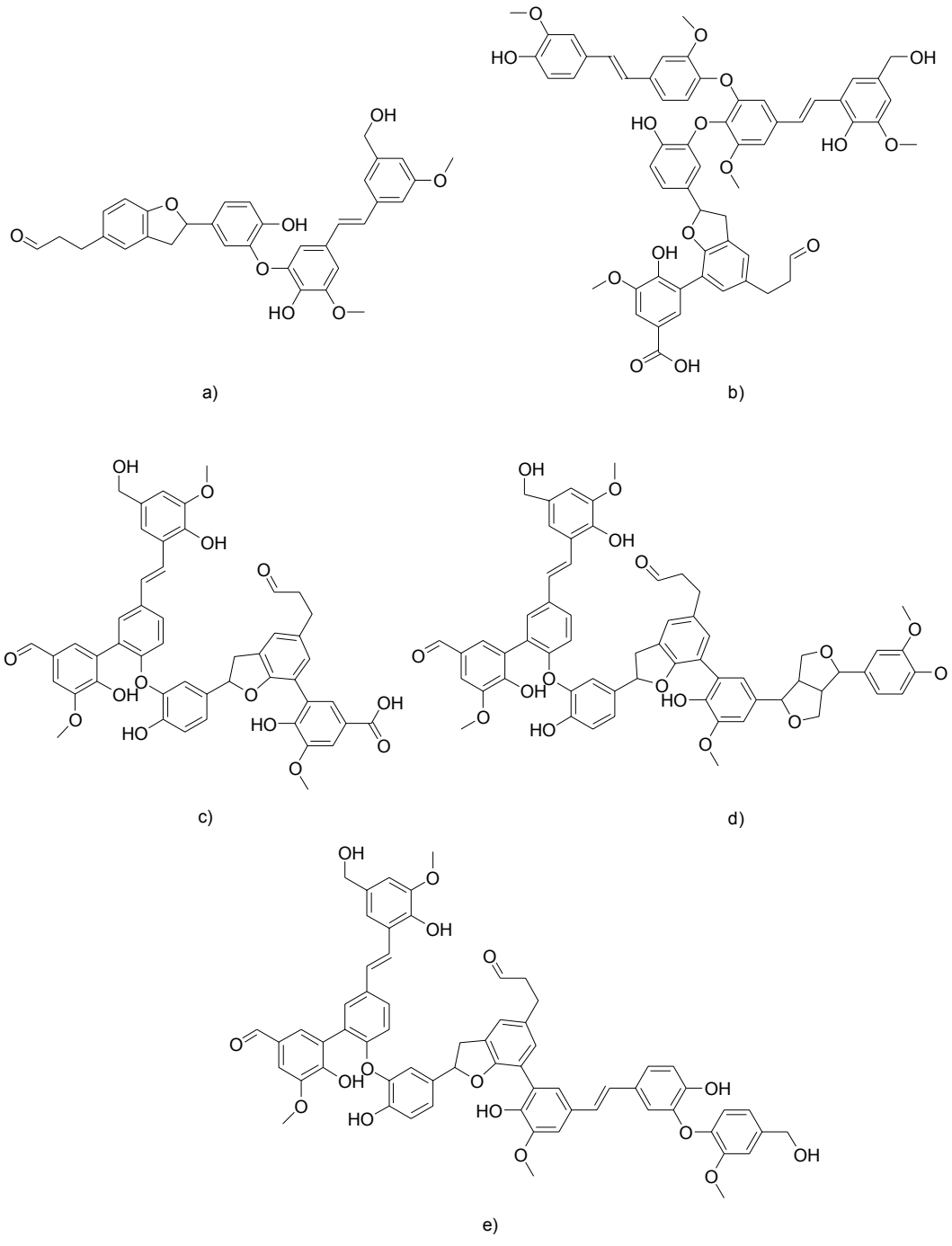

Figure 1.6 Oligomeric structures proposed for pyrolytic lignin: a) tetramer; b) pentamer; c) hexamer; d) heptamer; e) octamer (Bayerbach and Meier, 2009)

In a recent report, Bayerbach and Meier made an attempt to elucidate the chemical structure of the oligomeric molecules in pyrolytic lignin (Bayerbach and Meier, 2009). In this study, the carbon content determined by elemental analysis was found to be higher than that of milled wood lignin and technical lignins (Scholze and Meier, 2001). Based on their study, five generic structures of pyrolytic lignin were proposed based on tetramers to octamers of the phenylpropane moieties (**Figure 1.6**). These oligomers are typically characterized by biphenyl, phenyl coumaran, diphenyl ethers, stilbene and resinol structures (Bayerbach and Meier, 2009). According to these studies, the major differences between pyrolytic lignin and other technical lignin are that pyrolytic lignin has lower molecular weight (Scholze and Meier, 2001) and the aryl ether linkages prevalent in other technical lignins are absent in pyrolytic lignin (Bayerbach and Meier, 2009).

1.2 Carbon fibre

Lignin has been used in various applications (Glasser et al., 2000). One area of lignin utilization that is receiving increasing attention is the production of carbon fibres (Compere et al., 2001; Pickel et al., 2006). Carbon fibres are lightweight, high performance fibrous materials containing more than 90% carbon and exhibit imperfect graphite crystalline structures oriented along the fibre axis (Bahl et al., 1998). Carbon fibres are generally stronger yet lighter than most other structural materials (Fitzer, 1990); compared to steel and other metal fibres they possess much higher specific strength and moduli (**Figure 1.7**). There are basically two grades of high performance carbon fibres: HM (high modulus), also referred to as Type I; and HT (high strength),

referred to as Type II. Due to their superior properties, carbon fibres are widely employed in areas where high strength and lightweight are required. The composite materials made from carbon fibres are used in aircraft, rail vehicles, sporting equipment and various military applications (Bahl et al., 1998). Based on their lightweight and high strength, it is believed that the use of composites reinforced by carbon fibres in automotive parts could substantially decrease the fuel consumption of domestic vehicles (Compere et al., 2001; Pickel et al., 2006).

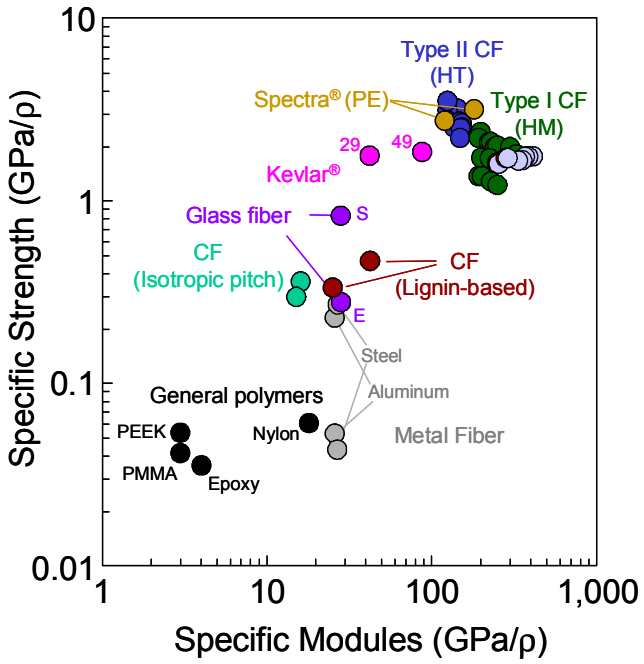

Figure 1.7 Specific Strength and modulus of typical fibers used in composite reinforcement

Carbon fibres can be made from any fibrous material that contain a carbon backbone (Bahl et al., 1998). However, the ideal precursor is one that is easily converted to carbon fibre with a high carbon yield at a relatively low cost (Morgan, 2005).

Although a number of naturally occurring polymers (cellulose, lignin) and synthetic fibres (polyester, phenolic resins, polyvinyl chloride etc.) have been investigated for the production of carbon fibre, only three precursor materials have been of commercial importance, namely, polyacrylonitrile (PAN), pitch (petroleum or coal tar), and viscose rayon (Bahl et al., 1998). Of these PAN and pitch have dominated the carbon fibre market owing to their superior properties and highly developed processing technologies. However, in recent years, rising petroleum costs and the increasing demand for high performance, lightweight composite materials, such as carbon fibres has resulted in the investigation of alternative renewable, less expensive and more widely available precursor materials. Some potential precursors under investigation, include lignin and various recycled plastics (Compere et al., 2001; Kadla et al., 2002b; Kubo and Kadla, 2005).

1.2.1 Carbon fibres based on polyacrylonitrile (PAN)

Among the three primary precursors, PAN has received most attention for developing high performance carbon fibres (Bahl et al., 1998).

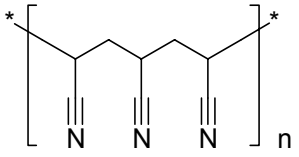

Figure 1.8 Chemical structure of polyacrylonitrile (PAN)

PAN fibres have a relatively high carbon yield, ~50–55% (Bahl et al., 1998; Morgan, 2005) which helps reduce the production cost per unit weight of product. As

well the chemical structure of PAN enables the polymer chains to develop a high degree of orientation during fibre spinning, which can be further improved through hot stretching and subsequent thermostabilization (TS). As a result PAN-based carbon fibres can possess tensile strengths of 3000 to 7000 MPa and Young's moduli of 200-600 GPa, and dominate the high performance aerospace and aviation markets.

Structurally, PAN has a continuous carbon backbone structure (**Figure 1.8**) with the nitrile groups situated in a position favorable for cyclization reactions. These are crucial steps in carbon production as they result in a ladder polymer believed to be the intermediate product towards the final structure of carbon fibre (*vide infra*).

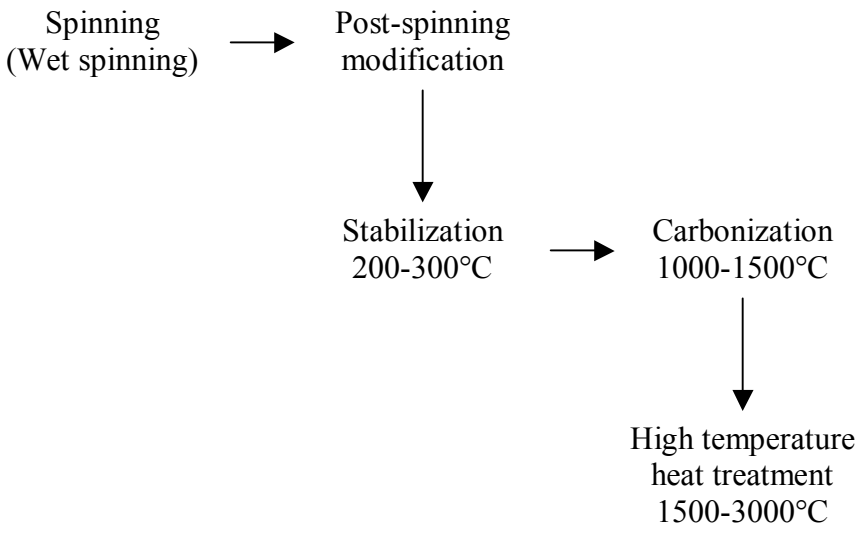

Figure 1.9 Major processing steps for production of PAN-based carbon fibre

Generally, there are five main processing steps (**Figure 1.9**) to make carbon fibres from PAN. In order to make carbon fibre, the raw material must be first made into fibres, which are usually referred to as "precursor", "white fibre" or "green fibre".

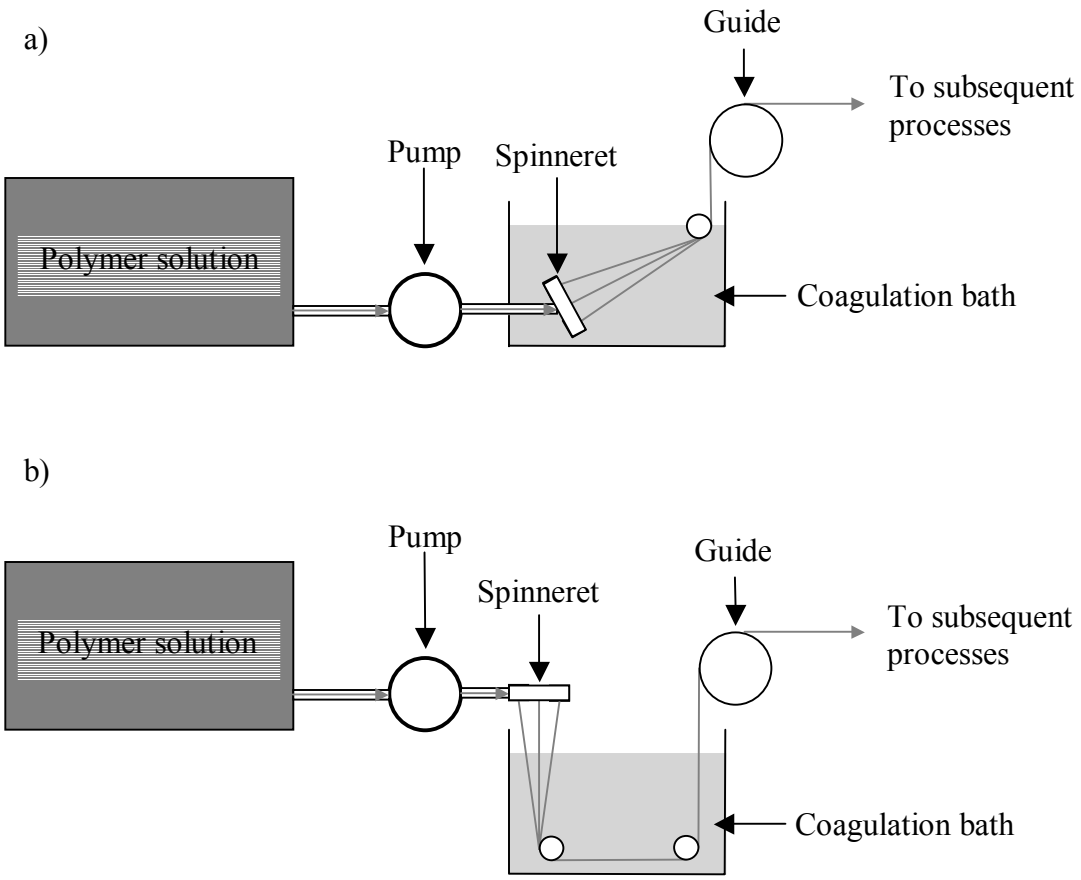

Figure 1.10 Schematic apparatus of a) wet spinning; and b) dry-jet wet spinning

There are a number of spinning methods by which PAN can be spun into white fibres, including wet spinning, dry spinning and melt spinning. Among these methods, the wet spinning of PAN has been the most used technique due to its high efficiency in spinning and high quality of resultant precursor fibres (Bahl et al., 1998). During the wet spinning process (**Figure 1.10 (a)**), the PAN polymer is dissolved in a solvent, such as Dimethylformamide (DMF) or Dimethyl sulfoxide (DMSO) to make a concentrated solution, known as a dope, which is then spun directly into a coagulation bath, typically an aqueous solution such as DMSO / H_2O system. In the coagulation bath, the PAN

fibres are in a swollen gel state, in which stretching of the PAN fibre leads to the unfolding of polymer chains and the development of molecular orientation (Nimts et al., 1986).

Currently the wet spinning technique is improved by letting the extruded PAN solution pass through air for a short distance (~10 mm) (Bahl et al., 1998) before entering the coagulation bath. This technique is generally known as dry-jet wet spinning (**Figure 1.10 (b)**). It allows the polymer chains to orient themselves through drawing in air before they enter the coagulation bath in which orientation is disrupted by diffusion of solvent. This feature further enhances the molecular orientation of PAN during spinning, leading to higher tensile properties of the PAN precursor fibres and hence the subsequent carbon fibres.

After spinning, modifications may be performed to boost the quality of precursor fibres. An example is post-spinning stretching with plasticizers like DMF, steam, nitrogen etc. to improve the fibre by manipulating the macromolecular structure of the PAN (Mathur et al., 1988; Chen and Harrison, 2002). After the post-spinning stretching, a reduction in fibre diameter results and leads to better mechanical properties as a result of the enhanced molecular orientation and decreased number of defects per unit volume.

Stabilization is the next step in carbon fibre production. It is usually conducted to render the fibres thermally stable to subsequent high temperature treatments, i.e. carbonization and high temperature heat treatment. In fact, it is regarded as the most critical step in carbon fibre manufacturing due to its strong effect on the final structure of

the fibre and hence ultimate mechanical properties (Bahl et al., 1998). Stabilization is also referred to as "thermostabilizaiton" or "thermo-oxidative stabilization" since this process involves heat treatment at lower temperature (with regard to carbonization temperature) under tension in an oxidative atmosphere. A typical stabilization for PAN is carried out in air at temperatures ranging from 180°C to 300°C with a heating rate of 1-2°C/min. This treatment induces changes in the chemical structure of the PAN precursor. Major reactions taking place are cyclization, dehydrogenation, and oxidation (Fitzer and Muller, 1975). The schematic representation of these reactions is given in **Figure 1.11** in which an oxidized ladder polymer is produced.

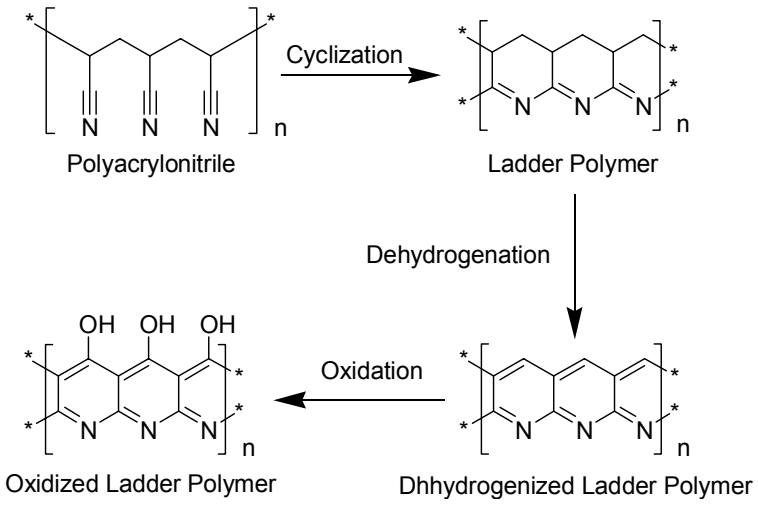

Figure 1.11 Chemical reactions involved in the thermostabilization of PAN precursor

In the process of carbonization, the stabilized PAN fibres are subjected to high temperature treatment under an inert atmosphere (usually nitrogen). The carbonization temperature is around 1500°C and the fibres may be carbonized under low or very little tension (Bahl et al., 1998). Most of the non-carbon elements are eliminated in this

process, leaving more than 90% carbon content in the carbonized fibres. A graphite-like structure starts to develop in the carbonization process (**Figure 1.12**).

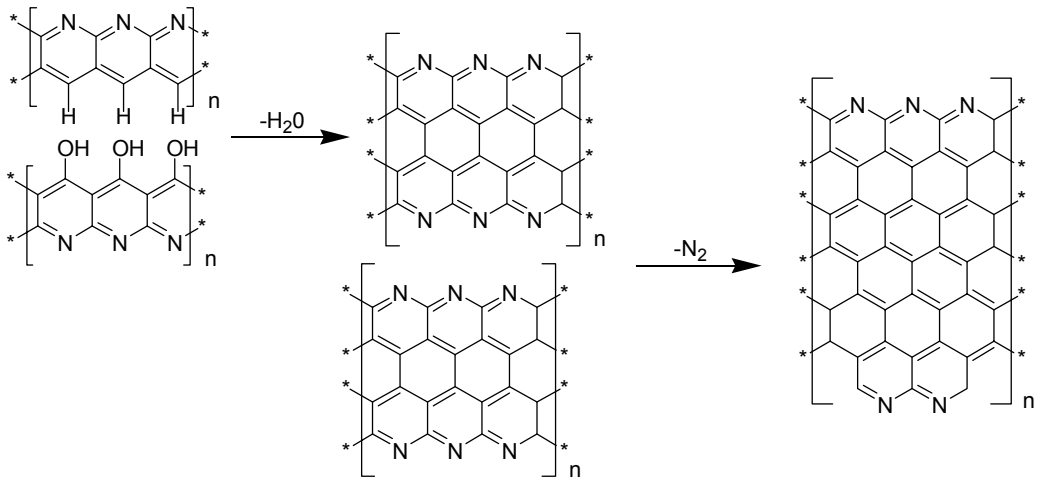

Figure 1.12 Formation of graphene sheet structure from precursor ladder polymer (stabilized PAN)

After carbonization, the fibres have a structure with small crystallites. Heating the fibres to temperatures beyond 1500°C, usually about 2000-2500°C and sometimes as high as 3000°C, in an inert atmosphere increases the size and crystalline perfection of the graphitic crystallites within the carbon fibres, as well as improves the crystallite alignment along the fibre axis (Bahl et al., 1998). The final carbon content is greater than 99% after the high temperature heat treatment (Pierson, 1993).

1.2.2 Carbon fibres based on pitch

Pitch-based carbon fibres offer excellent properties complementary to that of PAN-based carbon fibres. PAN-based carbon fibres are able to achieve high tensile strength at the cost of having moderate tensile modulus, whereas pitch-based carbon fibres generally

possess high modulus but with only moderate strength. Based on the properties of carbon fibres produced from pitch, two classes of carbon fibre are commercially available; i) general performance carbon fibre (GPCF), which has a tensile strength of up to 1 GPa and modulus of 40 to 50 GPa, and ii) high performance carbon fibre (HPCF), which has tensile strength up to 4 GPa and modulus from 180 to 900 GPa (Bahl et al., 1998).

Pitch is the by-product of the petroleum and coal-chemical industries (such as petroleum refined residue, coal tar pitch, the residue of solvent refined coal and petroleum). Depending on the specific pretreatment of the raw pitch material, there are two categories of precursor material for making carbon fibres – isotropic pitch and anisotropic pitch. Generally, isotropic pitch serves as the precursor for manufacturing general performance carbon fibre, whereas anisotropic pitch is the feedstock in making high performance carbon fibre (Morgan, 2005).

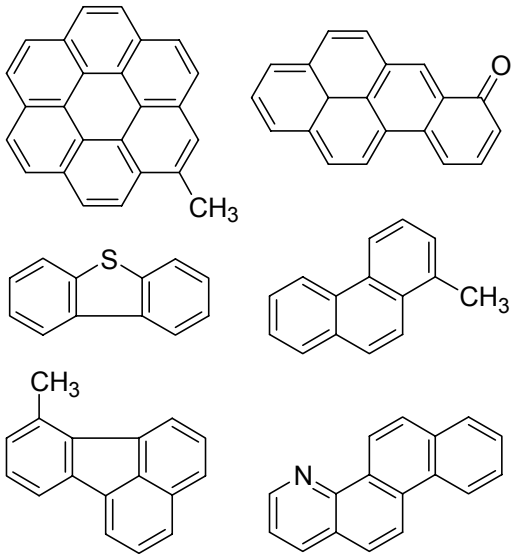

Figure 1.13 Representative structures of pitch (Morgan, 2005)

Pitch has a very complex structure and chemical composition (Bahl et al., 1998). It is a mixture of fused ring aromatic compounds with alkyl side-chains and heterocyclic compounds. **Figure 1.13** illustrates representative structures of pitch. It has a molecular weight ranging from 300 to 400 (Matsumoto, 1985); a carbon content of more than 80% and a softening point below 120°C (Bahl et al., 1998). At room temperature under normal conditions, it is a black shiny solid. The chemical composition and molecular weight distribution of pitch largely governs its properties. Albeit many types of industrial pitch exist, not all of them are suitable for manufacturing carbon fibres. Even those qualifying types of pitch are not readily transformed into carbon fibres with good quality. In order to optimize the quality of the raw pitch, it is necessary to make some adjustments and/or modifications.

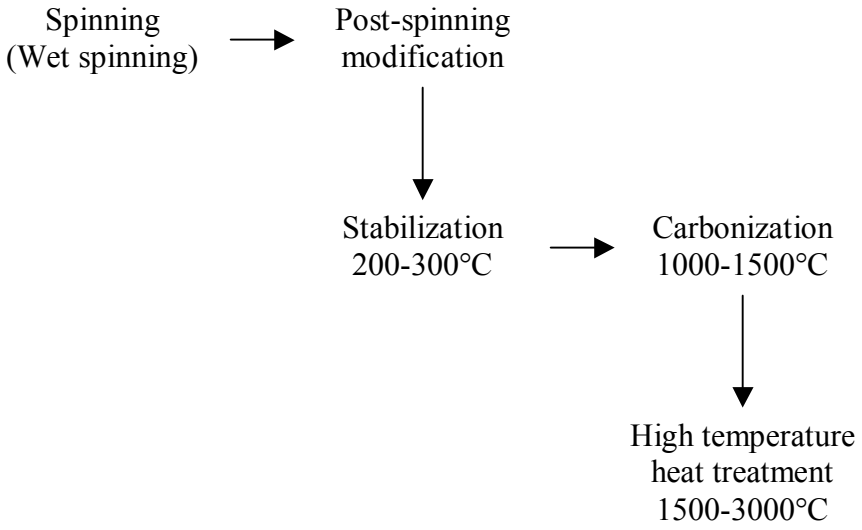

Figure 1.14 Major processing steps for production of pitch-based carbon fibre

The procedure for the production of carbon fibre from raw pitch (**Figure 1.14**) is similar to that from PAN, in that the precursor is spun into fibre form, thermostabilized

and finally carbonized / graphitized. However, unlike PAN, pitch requires a pretreatment stage. Due to the complexity of the chemical composition of raw pitch, it is necessary to refine pitch to get rid of impurities such as solids and primary quinolin insoluble matter. After refinement, the purified pitch typically has low ash, low heteroatom, and low metal ion content and high aromaticity. Industrial pretreatments or refinement methods are generally proprietary processes which usually involve multiple steps, including solvent refinement, distillation and super critical fluid extraction (Lisicki et al., 1988).

Although isotropic pitch and anisotropic pitch are derived from similar feedstock, they undergo quite different pretreatments prior to fibre spinning (Edie, 1990). For isotropic pitch, the purpose of pretreatment is to remove volatiles and increase the softening point of the pitch to prepare it for the subsequent melt spinning process. Pretreatment methods for isotropic pitch include thermal condensation (Bahl et al., 1998) and wiped film evaporation (Edie, 1990).

For anisotropic pitch, there are several pretreatment methods, including thermal modification (Park and Mochida, 1989), solvent modification (Diefendorf and Riggs, 1980), hydrogenation (Otani, 1982) and catalytic modification (Mochida et al., 1985; Mochida et al., 1990; Mochida et al., 1992). In all of these methods the principle motive is to generate and purify an oriented liquid crystalline mesophase, which is able to develop preferred alignment and orientation during melt spinning. It is this orientation that directly results in the high modulus required for high performance carbon fibre (Edie, 1990).

After pretreatment, the prepared pitch is then fed into an extruder where it is heated above its softening point and spun into fibres. By controlling the technical parameters of melt spinning (extrusion speed, orifice diameter, drawing speed, etc.), fibre diameter can be reduced to *ca.* 18 μm (Bahl et al., 1998). In addition, the spinning temperature (Morgan, 2005) and spinneret structure (Matsumoto, 1985) can effect the quality of the final pitch-based carbon fibres; higher temperatures leading to onion-radial traverse structures and lower temperatures leading to radial structures (**Figure 1.15**).

Images are not given here according to the Canadian copyright law. Please find the original images in the following reference:

Shen, Z., H. Guo, et al. (1996). Study on Structure and Performance of Graphite Fiber from Mesophase Pitch. Carbon and Carbonaceous Composite Materials: Structure-Property Relationships. K. R. Palmer, D. T. Marx and M. A. Wright. Singapore, World Scientific Publishing: 148-154.

Figure 1.15 SEM images of mesophase pitch-based carbon fibres produced from a) low (340^{o}C) and b) high (375^{o}C) fibre spinning temperature (Shen et al., 1996)

Pitch materials exhibit thermal-plasticity and soften upon heating above its softening point. Thus, at the high temperature of the carbonization and graphitization process, pitch fibres soften and fuse together, losing their fibre form. To avoid fusing, a thermostabilization process is also necessary prior to carbonization. During thermostabilization, oxidation and crosslinking reactions occur that change the thermoplastic character of pitch to a thermosetting character. As a result, thermostabilization increases the softening point of the pitch fibres, which are then

resistant to softening and fusion under the higher temperature conditions of the subsequent processing stages.

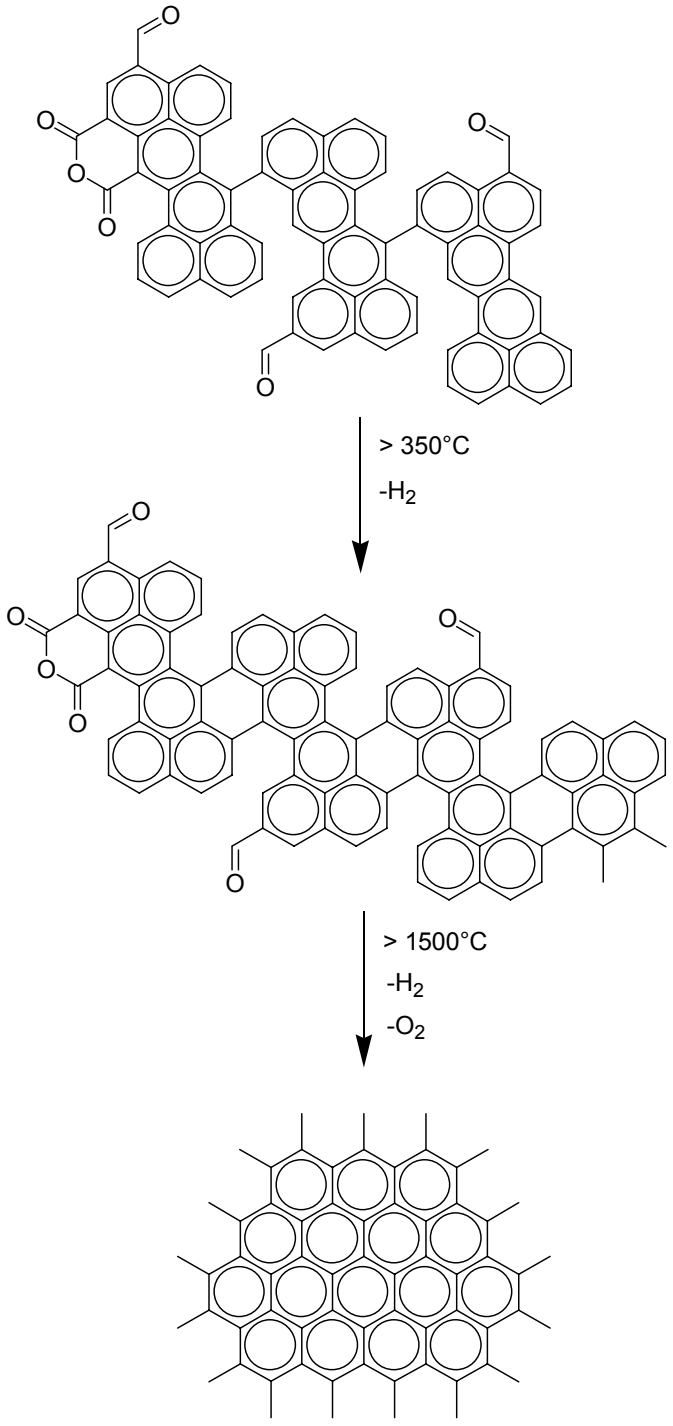

Figure 1.16 Schematic changes in pitch structure during carbonization (Bahl et al., 1998)

After stabilization, pitch fibres can be readily carbonized. Same as PAN fibres, carbonization of pitch fibres is usually performed between 1000 to 1600°C in an inert atmosphere (usually nitrogen), reaching carbon contents as high as 96% (Bahl et al., 1998). This process also leads to the formation of turbostatic graphite-like structures in the resultant fibres, thus improving their mechanical, electrical and thermal properties.

Figure 1.16 illustrates the change in chemical structure of pitch during carbonization (Bahl et al., 1998). Cross-linking and condensation start at the low temperature (<350°C) of carbonization process, giving off mainly H_2. In the temperature higher than 1500°C, the aromatic molecules of pitch fibres undergo further condensation and aromatization, giving rise to extended aromatic layers. In the mean time, Oxygen are eliminated from the fibre, generating O_2.

The properties of the pitch-based carbon fibres can be further improved through graphitization (high temperature treatment at 2000 to 3000°C). Under these conditions, the carbon atoms tend to form more stable structures, i.e. graphitic structures in which the carbon atoms are arranged in a hexagonal lattice separated by discrete distances; in pure graphite 0.142 nm between carbon atoms and 0.355 nm between lattice planes. As a result of graphitization, the perfection of the graphitic crystallites in the fibre is further improved and a structure close to that of ideal graphite is obtained. Thus, these graphitized fibres are usually termed “graphite fibres”, and can be differentiated from carbon fibres which have not undergone the graphitization treatment. As with melt spinning, the temperature of graphitization plays an important role in the mechanical properties of the final product. For graphite fibres based on anisotropic pitch, both tensile

strength and modulus increase with graphitization temperature, as high as 3 GPa and 900 GPa, respectively. This is different than that observed for isotropic pitch-based graphite fibres, which like PAN-based fibres show a decreases in tensile strength and increase in tensile modulus with the increasing graphitization temperatures (Matsumoto, 1985).

1.2.3 Carbon fibres based on lignin

Otani and colleagues (Otani et al., 1969) are considered among the first to report on the production of carbon fibres based on lignin. Using Kraft lignin, alkali lignin and lignosulfonate precursors, they compared the corresponding carbon fibres produced by melt and dry spinning. It was found that carbon fibres with better mechanical property were obtained by dry spinning of lignin dissolved in water, alkaline water and glycerol. The better mechanical properties can likely be attributed to the better orientation of lignin molecules in dry spinning as a result of relatively longer solidification time. They further observed that the blending of poly(vinyl alcohol) (PVA) and PAN with the lignin resulted in better spinning property and tensile strength. Shortly there after Mansmann et al. (Mansmann et al., 1973) dry-spun lignin-based fibres using an acidic solution and found that the acidic condition not only enhanced the mechanical properties of lignin fibre and resulting carbon fibre, but reportedly reduced the amount of synthetic polymer needed to improve fibre spinning property. Furthermore, they found that the acidic conditions reduced the temperature of thermostabilization to between 100-150°C. Following this pioneering work, pilot-scale production of lignosulfonate-based carbon fibre was pursued by Nippon Kayaku Co. Japan (Fukuoka, 1969; Mikawa, 1970) and marketed as Kayacarbon®. However, Kayacarbon® fibres were plagued with ubiquitous flaws and

lack of orientation within the fibres, resulting in low mechanical properties (Tomizuka et al., 1971; Tomizuka and Johnson, 1978). As a result, these carbon fibres were abandoned.

In the late 1980's and early 1990's Sudo and coworkers (Sudo et al., 1988; Sudo and Shimizu, 1992; Sudo et al., 1993) reported on the use of modified steam-exploded lignin as carbon fibre precursors. They reported that after hydrogenolysis or phenolation followed by solvent extraction and polycondensation under high temperatures the steam-exploded lignin was converted into a pitch-like molten material which was then processable into carbon fibres. The resultant carbon fibre showed superior mechanical properties to those of the Kayacarbon®.

Subsequently, Sano and colleagues (Uraki et al., 1995; Kubo et al., 1997; Kubo et al., 1998) prepared carbon fibres from Organosolv lignin obtained by aqueous acetic acid pulping. The softwood acetic acid lignin fibre was converted to carbon fibre without the need of a thermostabilization process, with properties suitable for mid-range performance carbon fibre markets. This is because lignin has a high oxygen content. The various hydroxyl and ether groups, via oxygen-based radicals, are anticipated to facilitate cross-linking between lignin molecules during the carbonization process, keeping the fibre integrity (Kubo and Kadla, 2006). However, as a non-commercial source of lignin this process did not proceed any further.

Recently, Kadla and colleagues (Kadla et al., 2002b) produced carbon fibre from an industrial Kraft lignin, without any chemical modification. It was found that the addition of as little as 1% poly(ethylene oxide) (PEO) greatly improved fibre fusion spinning.

These fibres had an overall yield of 45% and achieved tensile strengths of 400–550 MPa and modulus 30–60 GPa. Subsequent studies into the use of blending recyclable polymers with lignin, such as poly(ethylene terephthalate) (PET) and poly(propylene) (PP) (Kubo and Kadla, 2005) further enhanced carbon fibre properties, with tensile strengths and moduli of 600-700 MPa and 60-70 GPa, respectively. In addition it was found that immiscible lignin-polymer blends (e.g. lignin-PP) produce a porous carbon fibre morphology (Kadla et al., 2002a; Kubo et al., 2007) (**Figure 1.17**).

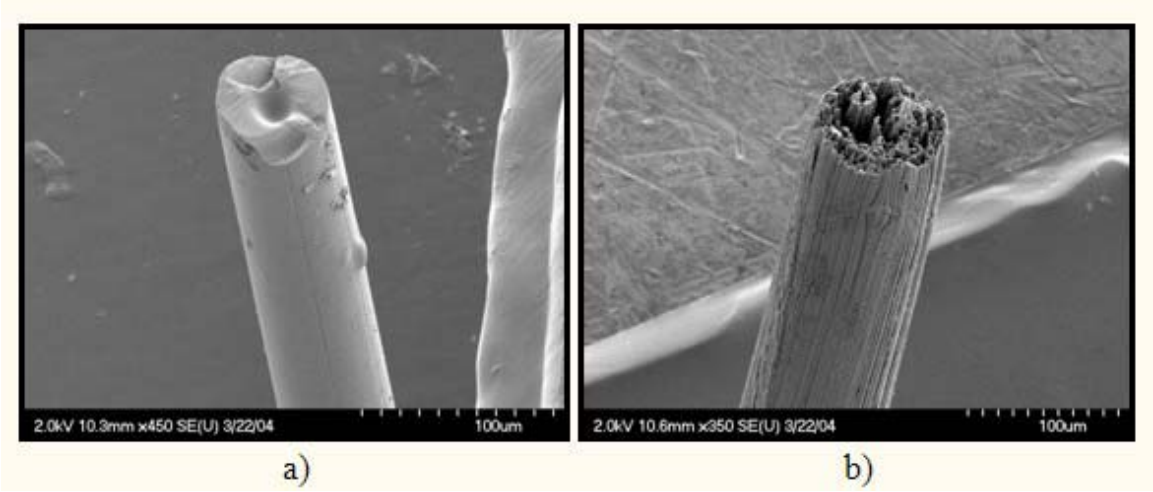

Figure 1.17 SEM images of lignin-based carbon fibres produced from Kraft lignin (a) and Kraft Lignin/PP blends (b) (Kubo et al., 2007)

1.3 Polymer/clay nano-composites

Polymeric materials have traditionally been reinforced using synthetic or natural inorganic fillers to improve mechanical properties. These materials have found wide use in various areas including transportation, construction, electronics and consumer products (Giannelis, 1998; Pavlidou and Papaspyrides, 2008). One of the most common

reinforcing materials is fibrous filler in a randomly dispersed state. Glass fibres, carbon fibres and natural biofibres (lignocellulosic fibres such as hemp, straw etc.) have all been widely utilized (John and Thomas, 2008). In fibre-reinforced composites, the applied load is transmitted and distributed among the fibres via the matrix. Significant reinforcement is possible provided the matrix-fibre bond is strong. Since reinforcement discontinues at the fibre ends, reinforcement efficiency depends on fibre length – the critical length depending on the fibre-matrix combination with both long and short fibres producing composite with unique properties. Fibre arrangement is also crucial relative to composite characteristics.

From a structural point of view, polymer-filler composites can be generally classified into '*conventional composites'* and '*nano-composites'*. In a conventional composite the registry of the filler is retained when mixed with the polymer, but there is no insertion of the polymer into the filler structure, i.e. intercalation (Figure 1.18). Consequently, the filler fraction in conventional filler-composites plays little or no functional role and acts mainly as a filler to reduce the amount of costly polymer use. An improvement in modulus is normally achieved, but this reinforcement benefit is usually accompanied by a reduction in strength or elasticity (Alexandre and Dubois, 2000).

The overall properties of composite materials are determined not only by the individual components, but also by the composite phase morphology and interfacial properties. In conventional composites phase mixing typically occurs on the macroscopic (μm) scale. If nanometre dispersion of the filler component can be achieved, enhanced performance properties can be obtained due to the unique phase morphology and

improved interfacial properties (Pinnavaia and Beall, 2000). Swellable clay minerals, although not nanometre-filler themselves, have been used to produce nanometre-sized filler when exfoliated within a polymer matrix. Generally, the larger the randomness of dispersion of clay platelets into the polymer matrix, i.e. exfoliation, the greater the enhancement of strength, stiffness and barrier properties. For these reasons, nano-structured organic-inorganic composites have attracted considerable attention from both a fundamental and applications point of view (Novak, 1993; Okada and Usuki, 1995).

Layered materials are well suited for the design of hybrid composites, because their lamellar elements have high in-plane strength and stiffness and a high aspect ratio (Pinnavaia, 1983). These attributes are shared among all families of lamellar solids, however, layered silicates have been the materials of choice for polymer nano-composites design. They exhibit a rich intercalation chemistry, which enables them to be chemically modified and made compatible with organic polymers for dispersal on the nanometre scale. As a result a vast amount of literature exists documenting the advantages of polymer/clay nano-composites.

Polymer layered silicate nano-composites were first reported in the patent literature as early as 1950 (Carter et al., 1950). Polyamide nano-composites were reported as early as 1976 (Fujiwara and Sakamoto, 1976). However, it was not until researchers at Toyota (Kawasumi et al., 1989) began a detailed examination of polymer layered silicate composites that nano-composites became more widely studied. Through in situ polymerization, the Toyota research group reported the preparation of nylon 6 clay nanocomposites exhibiting superior strength, modulus, heat distortion temperature as

well as water and gas barrier properties as compared with neat nylon 6 (Usuki et al., 1993). By adding only a small amount of organoclay, the density of the materials was not altered significantly, as was the case for mineral or glass fibres, thereby allowing it to be used for the first time for under-the-hood automotive applications. Today, there is an enormous amount of research being conducted into polymer/clay nano-composites owing to their novel properties. Polymer/clay nano-composites are not limited to a certain class of polymer; thermoplastic, thermosetting and even liquid crystalline polymer/clay nano-composites have been reported (LeBaron et al., 1999). Numerous studies have demonstrated that only a few percent of layered silicates can lead to increased stiffness and strength (Wang and Pinnavaia, 1998; Liu et al., 1999), improved solvent and UV resistance (Kojima et al., 1993; Huang et al., 2001), enhanced gas barrier properties (Yano et al., 1993; Messersmith and Giannelis, 1995; Nour, 2002), greater dimensional stability (Liu et al., 1999; Gu and Chang, 2001) and superior flame retardancy (Gilman, 1999).

In addition, clay has been reported to facilitate the graphitization of a number of polymers (Kyotani et al., 1988; Sonobe et al., 1988a; Sonobe et al., 1988b; Sonobe et al., 1990; Sonobe et al., 1991). In these reports, prior to carbonization, polymers were intercalated into the clay platelets without disrupting the regular parallel stacking of these platelets. It is believed that the parallel clay platelets provide the exact two-dimensional space for graphite formation thus help develop higher degree of crystalline perfection of the resultant graphitic material.

1.3.1 Dispersion of clay platelet within polymer matrix

Two types of polymer-filler nano-composites are possible: intercalated and exfoliated (**Figure 1.18**). Intercalated nano-composites are formed when one or a few molecular layers of polymer are inserted into the filler galleries with fixed interlayer spacing (d-spacing). Exfoliated nano-composites are formed when filler nano-layers individually dispersed in the polymer matrix, the average distance between segregated layers being dependent on filler loading, but typically separated by at least 10 nm. The separation between the exfoliated may be uniform (regular) or variable (disordered).

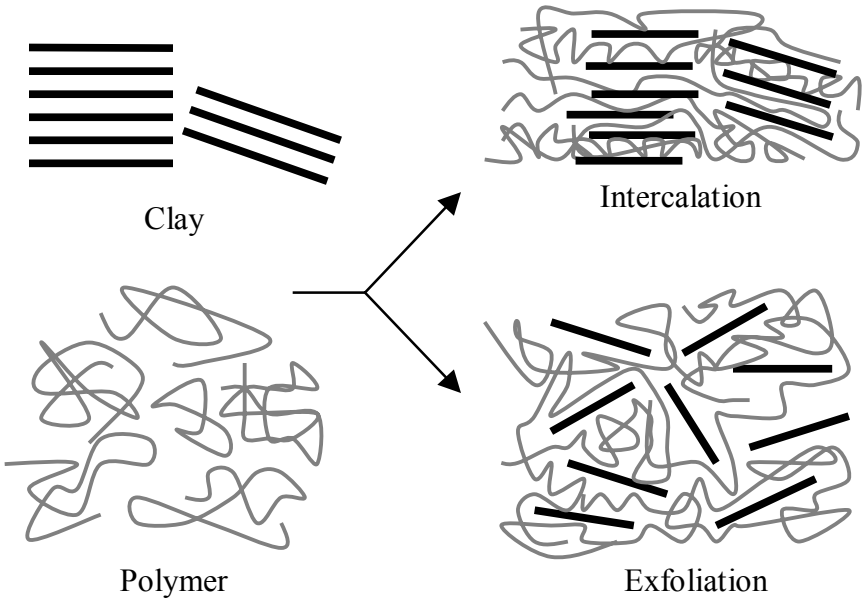

Figure 1.18 Schematic illustrations of the two types of morphology in polymer/clay nano-composites

Exfoliated nano-composites show greater phase homogeneity than intercalated nano-composites, and subsequently, contribute more to the interfacial interactions in the

matrix. The result is a more effective reinforcement and enhanced property performance of the filler-composite materials.

The enhancement in various properties is strongly influenced by the degree of dispersion of the clay platelets within the polymer matrices. Generally, higher degree of dispersion gives better the properties of the resultant nano-composite. Thus, a major concern in the preparation of polymer/clay nano-composites is the achievement of maximum dispersion of the nano-scale clay platelets into the polymer matrix (Goettler et al., 2007). In most polymer/clay nano-composite systems the achievement of intercalation is enough to observe property enhancement. However, exfoliation has been the ultimate goal of polymer/clay compounding since it is expected to bring dramatic improvements in nano-composite properties, as compared with intercalated nano-composites (Liu et al., 2006).

1.3.2 Preparation methods for polymer/clay nano-composite

As mentioned above, the key to the successful development of clay-based nano-composites is to achieve preferably exfoliation or at least intercalation of the clay layers of the polymer matrix. There are a number of methods available for preparing polymer/clay nano-composites: (i) *in-situ* polymerization (Kojima et al., 1993; Usuki et al., 1993; LeBaron et al., 1999; Zanetti et al., 2000), (ii) emulsion polymerization (Lee and Jang, 1998), (iii) sol-gel templating (Gu and Chang, 2001), and (iv) melt compounding (Vaia et al., 1993; Liu et al., 1999). A majority of the current nano-composite research has focused on nano-composites based on polymerization techniques,

i.e. methods i and ii. More recently, the advantages of polymer incorporation, whether through a sol-gel or melt compounding process, have evolved. As a result, nano-composites can be produced with higher filler incorporation and utilizing polymers not suitable for polymerization methods.

The sol-gel templating or solution intercalation method involves dissolving the polymer matrix and swelling the clay in a solution system, where the polymer chains enter and displace the solvent molecules within the galleries between clay layers (Zanetti et al., 2000). This requires a suitable solution system that can both dissolve the polymer and swell the clay. After removal of solvent and the nano-composite is formed.

In the polymerization intercalative techniques, a monomer is intercalated between the clay layers by mixing in a suitable solvent, and then polymerized within the clay galleries. The polymerization can be initiated by heat, radiation or various initiators. As a result, the polymer chains are formed between the clay galleries, which are intercalated and expanded (Ray and Okamoto, 2003).

In melt compounding, the polymer/clay mixture thermally extruder under shear, typically above the softening point of the polymer (Zanetti et al., 2000). During this process, the molten polymer diffuses into the clay galleries, forming either intercalated or exfoliated structures depending on the degree of desperstion (Nam et al., 2001). Compared with the aforementioned two methods, melt compounding is much simpler and applies to many polymers as long as they are melt-processible. It allows the use of polymers which were not suitable for in-situ polymerization or sol-gel intercalation due

to solubility issues. Moreover, it is environmentally benign in that it does not involve any organic solvents and is compatible with current industrial processes, such as extrusion and injection moulding. As a result, melt compounding has become the mainstream for the preparation of polymer/clay nano-composites (Zanetti et al., 2000).

1.4 Motivation

Pyrolytic lignin is reported to have a negative impact on the quality of bio-oil; it reduces bio-oil stability and combustion efficiency (Bayerbach and Meier, 2009). Thus, to improve the value and properties of bio-oil it is desirable to remove the pyrolytic lignin. However, the separation of pyrolytic lignin, bio-oil upgrading will have a cost associated with it. Moreover, a potentially large volume of pyrolytic lignin may be generated, which may further introduce additional costs, for handling / disposal, as well as impact on the environmental. Therefore, it is necessary to find value-adding applications for pyrolytic lignin.

Carbon fibre production is a potential application for pyrolytic lignin. Due to the extremely low density and high strength, it is believed that the use of composites made from low-cost carbon fibre in automotive parts could substantially decrease the fuel consumption of vehicles (Compere et al., 2001; Pickel et al., 2006). However, current economics preclude the utilization of carbon fibre in automobile applications; the current precursors PAN and pitch are too expensive and cannot be produced in sufficient quantities to meet the automotive sector needs (Compere et al., 2001). As neither of the two major precursors for making carbon fibres, PAN and petroleum pitch are renewable

materials, issues surrounding sustainability also exist. Lignin is the second most abundant polymer on earth; it is renewable and relatively inexpensive. Lignin is a promising alternative feedstock for the production of low-cost carbon fibre.

Thus, the production of carbon fibre from pyrolytic lignin will not only add value to pyrolytic lignin, but also reduce the price of carbon fibre, thereby opening new opportunities for advanced composite use. This thesis investigates the production of carbon fibre from pyrolytic lignin as well as the impact of organoclay reinforcement on the mechanical properties of the resulting pyrolytic-lignin-based carbon fibres.

1.5 Hypothesis

1.5.1 Pyrolytic lignin can be used to make carbon fibre

As mentioned in the introduction chapter, pyrolytic lignin and technical lignins have relatively similar structures. Since technical lignins are potential feedstock for making general purpose carbon fibres (Compere et al., 2001; Pickel et al., 2006), pyrolytic lignin should also be considered among these potential precursors. Moreover, there are two advantages for pyrolytic lignin over other technical lignins as carbon fibre precursor: i) Pyrolytic lignin has a relatively lower molecular weight (Scholze et al., 2001) and is thus easier to be spun into fibres; ii) Pyrolytic lignin has higher carbon content which may result in higher carbon yield and hence lower cost of carbon fibre.

1.5.2 Organoclay can enhance pyrolytic-lignin-based carbon fibre

Clay or layered silicates are popular reinforcing agents for various polymer systems (Giannelis, 1998; Pavlidou and Papaspyrides, 2008). A few percentages of clay loading can lead to dramatic improvements in mechanical, thermal and barrier properties (Giannelis, 1998; Pavlidou and Papaspyrides, 2008). Incorporation of clay has also been reported to facilitate the formation of graphitic structure from a number of polymers (Kyotani et al., 1988; Sonobe et al., 1988a; Sonobe et al., 1988b; Sonobe et al., 1990; Sonobe et al., 1991). It is believed that clay helps develop more ordered graphitic structure which give rise to better mechanical properties. It is therefore hypothesized that the reinforcement of lignin-based fibres with organoclays can improve the mechanical properties of lignin fibre as well as the resultant carbon fibre.

1.6 Thesis outline

This work consists of two parts. The first part focuses on examining the possibility of producing carbon fibres from pyrolytic lignin; the second one evaluates the effect of organoclay reinforcement on the properties of the carbon fibre produced from pyrolytic lignin.

2 MATERIALS AND METHODS

2.1 Materials

2.1.1 Bio-oil and pyrolytic lignin

Bio-oil was made from mixed hardwood sawdust by Dynamotive Energy Systems Corporation. It was kept in the dark at 4°C upon received to prevent side reactions (Scholze and Meier, 2001).

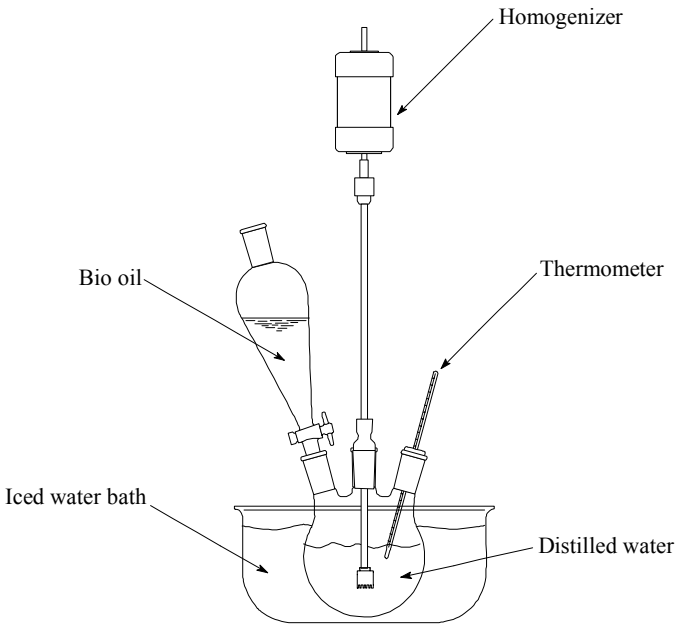

Figure 2.1 Schematic illustration of the experimental set-up for the separation of lignin from bio-oil

Pyrolytic lignin was isolated from bio-oil according to the literature (Scholze and Meier, 2001). Specifically, 500 ml bio-oil was added drop-wise (~10 ml/min) to 15L cool de-ionized water (kept in an ice-water bath) while being stirred with a homogenizer at

7000 rpm (**Figure 2.1**). Oil / water volume ratio of 1 : 30 was chosen for lignin isolation. Phase separation of the bio-oil began immediately upon introducing the bio-oil into the agitating water. It is observed that when using oil / water volume ratio higher than 1 to 30, the phase separation of bio-oil droplets could not occur immediately, which led to the conglomeration of bio-oil and hence ineffective lignin isolation.

Figure 2.2 Photo of pyrolytic lignin isolated in this work

The water insoluble fraction that precipitated from the system was collected by vacuum filtration using Fisherbrand Grade P8 qualitative filter paper (Cellulose fiber, 24.0cm in diameter), and thoroughly washed with 3L de-ionized water. After freeze-drying, a light-brown fine powder (pyrolytic lignin) was obtained (**Figure 2.2**). The yield of pyrolytic lignin is 22.3 wt%.

The pyrolytic lignin was thoroughly characterized and the structural information is tabulated in **Table 2.1** and **Table 2.2**. Based on the elemental and functional group analysis an empirical C_9 formula of pyrolytic lignin was also calculated (**Table 2.2**). The

functional group content of pyrolytic lignin used in this work is similar to that reported in the literature (Scholze and Meier, 2001; Bayerbach and Meier, 2009).

Table 2.1 Pyrolytic lignin structural information

Functional Groups (mmol/g)			Molecular Mass		Thermal Analysis	
Hydroxyl		Methoxyl				
Aliphatic	Phenolic		M_w	PDI	T_g (°C)	T_d (°C)
1.7	6.0	2.3	702	2.3	70	150

M_w: Weight average molecular weight; PDI: Polydispersity index; T_g: Glass transition temperature; T_d: Decomposition temperature

Table 2.2 Elemental composition and empirical formula of pyrolytic lignin

Elemental Composition (%)			Empirical C_9 Formula
C	H	O	
67.1	5.9	26.7	$C_9 H_{7.38} O_{1.12} (OCH_3)_{0.39} (OH_{phon})_{1.01} (OH_{aliph})_{0.29}$

2.1.2 Technical lignins

Organosolv lignin (Alcell®) was obtained from Repap Enterprises Inc. and used as received. Kraft lignin was obtained from MeadWestvaco Corp (Charleston, SC). The Kraft lignin samples were desalted as per our previous work (Kadla et al., 2002b). Specifically, 50g of Kraft lignin was washed 3 times with 2L distilled water while

maintaining the pH below 5 using HCl. The lignin was then air-dried and collected as fine powder.

2.1.3 Organoclays

Two types of organically-modified montmorillonite (MMT) organoclays, Cloisite® 30B and Cloisite® 20A were purchased from Southern Clay Co. (Austin TX, USA) and used as received.

Table 2.3 Organoclay structural information

Organoclay	Organic Modifier[a]	2 Theta Angle (degree)	Interlayer Spacing (nm)
Cloisite® 20A	$(CH_3)_2(HT)_2N^+$	3.48	2.54
Cloisite® 30B	$(CH_3)(T)(CH_2CH_2OH)_2N^+$	4.67	1.89

[a]: T: tallow, HT: hydrogenated tallow

The structures of the interlayer counterions of the two types of organoclays used in this study are listed in **Table 2.3**. Both are quaternary ammonium cations with slightly different organic components. The Cloisite® 20A has 2 methyl and 2 hydrogenated tallow groups (hydrogenated tallow groups are saturated hydrocarbons with various number of carbon atoms from 14 to 18) making up its quaternary ammonium component. By contrast the Cloisite® 30B has only one methyl group, one tallow group (unstturated hydrocarbon chains with 14 – 18 carbon atoms) and two hydroxyethyl groups as part of its ammonium centre.

2.2 Preparation methods

2.2.1 Thermal pretreatment

Thermal pretreatment was performed in a modified gas chromatography oven (Hewlett Packard HP 5890 Series II). Around 15g of pyrolytic lignin powder was contained in a 250 ml sealed round-bottom flask which was connected to house vacuum (~ 30KPa). After evacuation of the flask, the temperature was increased at 30°C/min to the desired temperature and held for a period of time depending on the treatment conditions. Alcell lignin and Kraft lignin were both treated at 160 °C for 30 minutes at ~ 30KPa prior to fibre spinning as per previously reported (Kadla et al., 2002b; Kubo and Kadla, 2005). The pyrolytic lignin samples used for organoclay reinforcement were treated at 160°C for 1 hour at ~ 30KPa (see section 3.1).

2.2.2 Mechanical mixing, melt compounding and fibre spinning

To reinforce pyrolytic lignin, the organoclay and pretreated lignin powder (10g in total) were mechanically mixed in a Retsch PM 200 ball-mill at 500 rpm for 30 minutes under Argon atmosphere. A 45-ml zirconium dioxide bowl with 6 stainless steel balls (1 cm in diameter) was used. These pyrolytic lignin/organoclay mixtures were then thermally extruded into pellets, which were then re-extruded and spun into the fibre form using a Dynisco® Laboratory Mixing Extruder (Atlas Electric Devices Co.) equipped with a ca. 0.8 mm spinneret.

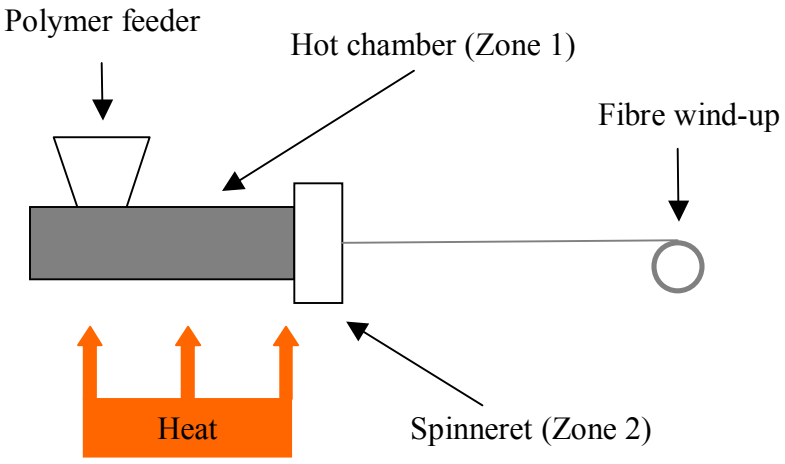

Figure 2.3 Schematic of the melt spinning apparatus used in this work

The spinning apparatus is depicted in **Figure 2.3**. Pyrolytic lignin was fed into the hot chamber (Zone 1) where it is heated to the predetermined spinning temperature (from 105 to 180°C) and pumped into the spinneret (Zone 2) which was also heated at a predetermined temperature. The resultant extruded lignin fibre was collected on spools by a take-up device (Atlas Electric Devices Co.). The optimal conditions for fibre spinning were obtained by slowly increasing temperatures in both heating zones and adjusting the take-up speed until continuous fibre spinning was achieved (Kadla et al., 2002b; Kubo and Kadla, 2005).

2.2.3 Thermostabilization and carbonization

Thermostabilization was performed as per the literature (Kadla et al., 2002b) using a modified gas chromatography oven (Hewlett Packard HP 5890 Series II). Lignin fibres were heated in air at a rate of 0.5°C/min to 250°C, and then held at 250°C for an hour. In order to induce molecular orientation, the fibres were thermostabilized under tension by

fixing the two ends of the fibre onto a clamping system. The thermostabilized fibres were then carbonized in a GSL1100X tube furnace (manufactured by MTI corp.) under a nitrogen atmosphere by heating from 25-1000 °C at 3°C/min and held for one hour at 1000 °C (fibres not under tension due to the limitation of the carbonization equipment available).

2.3 Characterization methods

2.3.1 Chemical characterization

^{1}H and ^{13}C NMR were measured using a Bruker Avance 300MHz spectrometer equipped with a BBO probe. For quantitative ^{1}H NMR, 15 mg of acetylated lignin was accurately weighed and dissolved in 0.5 mL deuterated chloroform. 2 mg of 4-nitrobenzaldehyde was added into the solution as internal standard for quantitative determination of functional group content. The NMR spectra were recorded at 25°C, with a 90º pulse width and a 1.3 s acquisition time. A 7 s relaxation delay (d1) was used to ensure complete relaxation of the aldehyde protons. A total of 128 scans were collected. Quantitative ^{13}C NMR spectroscopy was performed using a lignin concentration of 15 wt% in DMSO-d_6. The sample solutions were filtered prior to NMR analysis. Relaxation was facilitated by the addition of 10 μL of a chromium acetoacetonate solution (final concentration 10 mM) (Capanema et al., 2004). Conditions for analysis included a 90º pulse width with a 0.9 s acquisition time and a 1.7 s of relaxation delay (d_1). A total of 80,000 scans were collected.

The methoxyl and hydroxyl group contents were calculated from the quantitative ^{1}H NMR spectrum of acetylated pyrolytic lignin. Acetylation was performed by dissolving 200 mg of pyrolytic lignin in 8 mL of pyridine/acetic anhydride (1:1, v/v) and stirring the reaction for 48 h at room temperature. The reaction solution was then added dropwise with stirring to 300 mL of ice-water. The precipitated lignin was collected by filtration through a Nylon membrane (0.45 μm, 47 mm), washed with 3L ice-cold distilled water, and freeze-dried using a VirTis EX freeze-dryer. Complete acetylation was confirmed by FTIR spectroscopy.

Elemental analysis was performed by the UBC Mass Spectrometry and Microanalysis Centre using a Carlo Erba Elemental Analyzer (EA 1108). C, H, N contents were directly determined whereas the O content was calculated by difference.

2.3.2 Molecular weight determination

The relative average molecular weight distribution of the pyrolytic lignin preparations were determined by Gel permeation chromatography (GPC; Agilent 1100, UV and RI detectors) using styragel columns (Styragel HR 4 and HR 2) at 35 °C with THF as the eluting solvent (0.5 mL min^{-1}) and UV detection at 280 nm. Pyrolytic lignin concentration was 1 mg mL^{-1} and the injection volume was 100 μL. Polystyrene standards are used for the calibration.

2.3.3 Thermal analysis

Thermal analyses of the untreated and treated lignin samples were performed by thermogravimetric analysis (TGA) and differential scanning calorimetry (DSC) using a TA Q500 TGA and TA Q1000 DSC, respectively. In thermogravimetric analysis, 5-10 mg samples were heated from 40°C to 1000°C in nitrogen at a heating rate of 20°C/min. The decomposition temperature (T_d) of all samples was determined as the temperature at which 5% weight loss of the sample were measured. Values of T_d are reported as the average of 3 replicates, with coefficient of variance less than 2%. DSC analyses were conducted under a nitrogen atmosphere using approximately 3mg of sample in each run. The samples were heated from 20°C to 120°C at a heating rate of 10 °C/min (first heating run), then cooled to 0°C at 5 °C/min (cooling run) and subjected to a seconding heating from 0°C to 200°C (second heating run) at 10°C/min. The glass transition temperature (T_g) of the samples were measured as midpoint temperatures of the step change in heat capacity on the heat flow curve of the second heating run. Values of T_g are reported as the average of 3 replicates, with coefficient of variance less than 1%.

2.3.4 Wide-angle X-ray diffraction

Wide-angle X-ray diffraction (WAXD) experiments were performed using a Bruker D8 Discover X-ray diffractometer with Cu Kα radiation operated at 40 kV and 40 mA. Diffraction patterns were collected for well aligned fibre bundles (each bundle consisted of approximately 50 fibres of 20mm in length) using an area array detector. For the pure organoclay, WAXD samples were prepared using a molding-press device for Infrared

spectroscopy sampling; 200mg organoclay powder was compressed at 8000 psi for 5 minutes and molded into a thin disc. For all samples a total data collection time of 100 seconds was used.

2.3.5 Scanning electron microscopy

Micrographs of gold-coated fibres were taken on a Hitachi S-3000N scanning election microscope (SEM). The accelerating voltage was 20kV; and magnification varied from ×100 to ×1000.

2.3.6 Yield measurement

The yield after each processing step, except for the spinning yield, was determined by weighing the samples before and after the production step. However, due to the experimental set-up it was not possible to use this protocol to measure the spinning yield, therefore, thermogravimetric analysis (TGA) was employed. In the TGA experiments, the corresponding lignin preparation was first heated to its spinning temperature (zone 1) in one minute and then heated to the zone 2 spinning temperature in 5 minutes (estimated resonance time) to simulate fibre spinning.

2.3.7 Tensile testing

The tensile strength, modulus and elongation of the individual carbon fibres were measured according to the ASTM standard C1557-03(2008) with an Instron® Tension Tester (model 5565) using a gauge length of 25 mm. Data are reported as the average of

20 fibres per sample. Fibre diameters were determined using a calibrated optical microscope, and are reported as an average of three measurements along the fibre. Tensile strength and modulus values are reported as averages ±95% confidence interval using a *T*-statistic. One-way analysis of variance (ANOVA) was performed to the result of tensile test by Tukey multiple comparison at 5% significance level.

3 RESULTS AND DISCUSSION

3.1 Carbon fibre from pyrolytic lignin

It is reported that using carbon fibre composites in automobile parts will dramatically decrease fuel consumption by lowering overall weight of vehicles (Compere et al., 2001; Pickel et al., 2006). However, the high price and moderate availability of current carbon fibre precursors limit their applications. Therefore, there is a need to find alternative low cost, large volume feedstock materials. Lignin is regarded as a potential feedstock for low-cost carbon fibre production due to its moderate price and high volume availability (Compere et al., 2001). A number of technical lignins have been investigated as carbon fibres precursor. These lignin feedstocks include steam explosion lignin (Sudo and Shimizu, 1992; Sudo et al., 1993), acetic acid lignin (Uraki et al., 1995; Kubo et al., 1998), Alcell lignin (Kadla et al., 2002b) and Kraft lignin (Kadla et al., 2002b; Kubo and Kadla, 2005).

Pyrolytic lignin is also a potential precursor for the production of low-priced carbon fibres. It is the water insoluble fraction of bio-oil and is removed from bio-oil in the process of bio-oil upgrading. To make this upgrading process more profitable and environmentally friendly, it is necessary to find value-adding application for the co-product of this process – pyrolytic lignin. One potential application for pyrolytic lignin is to use pyrolytic lignin as the precursor for carbon fibre production.

This section focuses on the production of carbon fibre from pyrolytic lignin, specifically, the pretreatment of pyrolytic lignin, yield and mechanical properties of resultant carbon fibre. Also included for comparison is the production of carbon fibres from Kraft and Alcell lignin. All carbon fibres were produced using essentially the same processing conditions, the only difference lies in the pretreatment condition which plays an important role in the carbon fibre production from pyrolytic lignin.

3.1.1 Effect of pretreatment conditions on the production of carbon fibre

Pyrolytic lignin along with Kraft and Alcell lignins were readily spun into fibres through melt spinning. **Table 3.1** lists the temperatures for the first and second heating zones required to enable continuous fibre spinning. Also included in **Table 3.1** is the corresponding glass transition temperature (T_g) as well as molecular weight for the respective lignins. The temperatures required for continuous fibre spinning of the pyrolytic lignin was lower than those needed for both Kraft and Alcell lignin. One reason for the relatively lower spinning temperature of pyrolytic lignin is its lower relative average molecular weight, which increases the free volume and lowers the T_g (Larrain et al., 1981). The lower T_g corresponds to a lower softening point (Brydson, 1999) and subsequent lower fibre spinning temperatures.

With proper control of spinning temperature and size of the spinneret, lignin fibres with diameters as small as 20 μm could be obtained using pyrolytic lignin. These fibres were smaller than the minimal diameter obtained from both Alcell and Kraft lignin, 30 and 50 μm respectively. Continuous spinning of the pyrolytic lignin for over 20 minutes

was easily achieved. The improved spinning properties, defined as the ability of the polymer to achieve continuous spinning)[0] of the pyrolytic lignin, as compared with Alcell and Kraft lignin, may again be attributable to its low molecular weight, inherent chemical structure and thermal properties.

Table 3.1 Spinning temperature and glass transition temperature of pyrolytic, Alcell, and Kraft lignin

Lignin type	Spinning Temperature* (°C)		T_g (°C)	M_w (PDI)
	Zone 1	Zone 2		
Kraft	170	202	131	1256 (2.2)
Alcell	130	158	77	790 (2.5)
Pyrolytic	105	125	70	702 (2.3)

*: Spinning temperature for each type of lignin was recorded when continuous fibre formation was achieved; T_g: glass transition temperature; M_w: weight average molecular weight; Mn: number average molecular weight; PDI: Polydispersity index: ratio of M_w/M_n

However, SEM analysis of the pyrolytic lignin fibres revealed a very unique microstructure (**Figure 3.1 (a)**). The pyrolytic lignin fibres were found to contain large quantities of voids and cavities. This porous fibre morphology will significantly impact the mechanical properties of the resultant carbon fibre (Kadla et al., 2002a). These large voids likely arise by the gasification of volatiles in pyrolytic lignin during the fusion spinning process. As outlined above (**Table 1.2**), bio-oil and thus the resulting pyrolytic lignin (water insoluble fraction) contain a large variety of chemical constituents. It is

likely that these volatile organic components flash off during the thermal processing of fusion spinning, resulting in the voids and discontinuous fibre morphology.

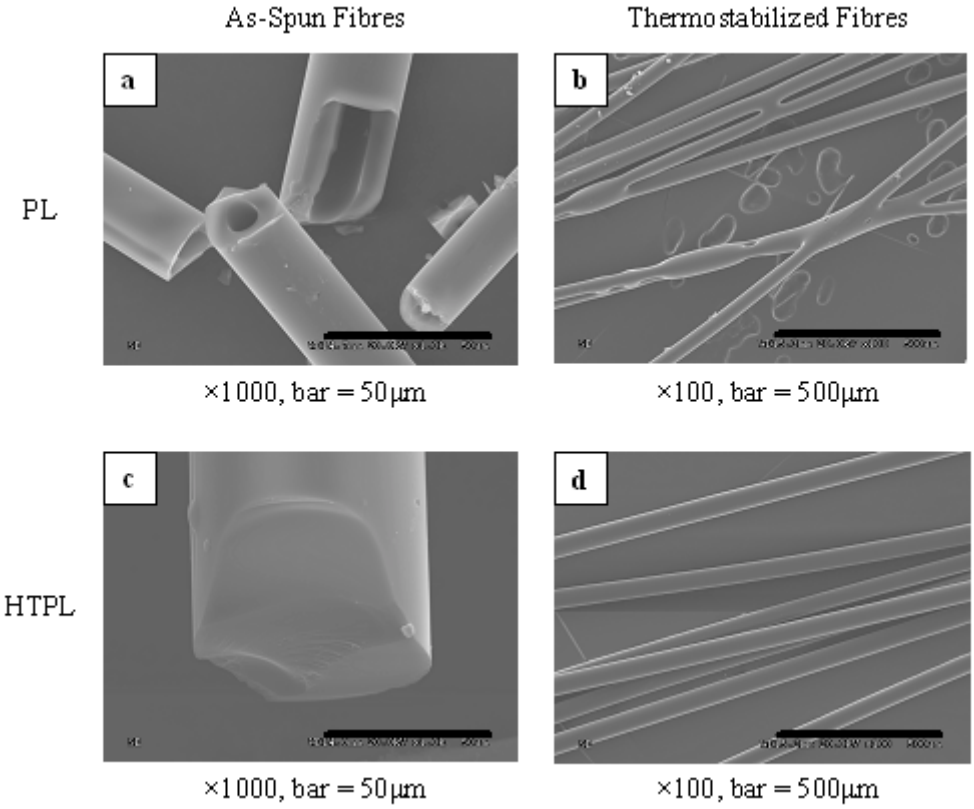

Figure 3.1 SEM micrographs of a) as-spun pyrolytic lignin (PL) fibres; b) thermostabilized pyrolytic lignin fibres; c) heat-treated pyrolytic lignin fibres (HTPL: lignin pretreated at 160°C for 1 hour at 30 KPa prior to spinning) and d) thermostabilized heat-treated pyrolytic lignin fibres

Thermogravimetric analysis (TGA) of the pyrolytic lignin provides evidence of volatile components, as revealed by the subtle change in the derivative (DTG) weight loss curve after fibre spinning (**Figure 3.2**). The small peak (corresponding to ~ 4% weight loss) at ~ 100°C in the DTG curve likely corresponds to the volatile components within

the pyrolytic lignin, which after spinning, reduces in intensity and evolves into two peaks: one at ~ 70°C (2% weight loss); the other ~ 110°C (1% weight loss). This observation coincides with the gasification of volatiles during the temperatures utilized in fibre spinning ~105-125°C and might be responsible for the formation of large cavities in the as-spun fibres. Similarly, there is a large change in the DTG profile after thermostabilization during which the pyrolytic lignin experienced higher temperature (250°C) for longer time (1h) relative to the spinning process. Showing less than 0.3% in weight loss, the peak corresponding to volatile components within pyrolytic lignin almost disappears after thermostabilization. There is also an enrichment/enhancement of higher temperature degrading material > 400 ^{o}C.

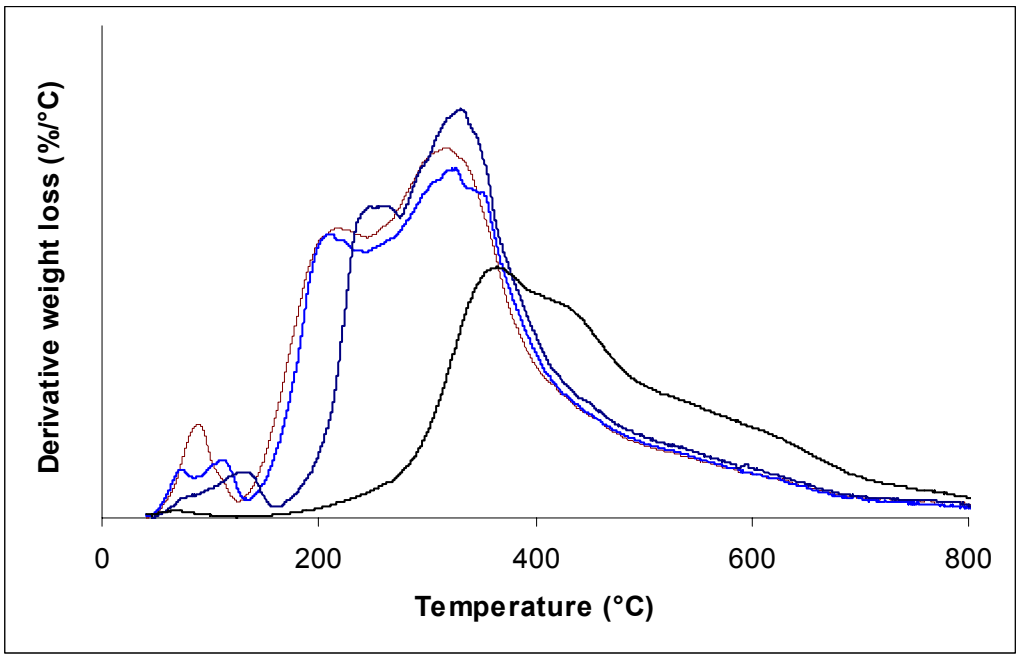

Figure 3.2 DTG curves of pyrolytic lignin before (dark red) and after (blue) spinning, after thermostabilization (black), and pyrolytic lignin pretreated at 160°C for 1 hour at 30KPa (dark blue)

Since the lignin sample may absorb a certain amount of water before the TGA experiment, the observed volatile peak at ~ 100°C might also be a result of absorbed water. However, gas chromatography analysis (data not shown) showed the presence of numerous low molecular weight volatile compounds, clearly indicating that water is not the only volatile component in pyrolytic lignin.

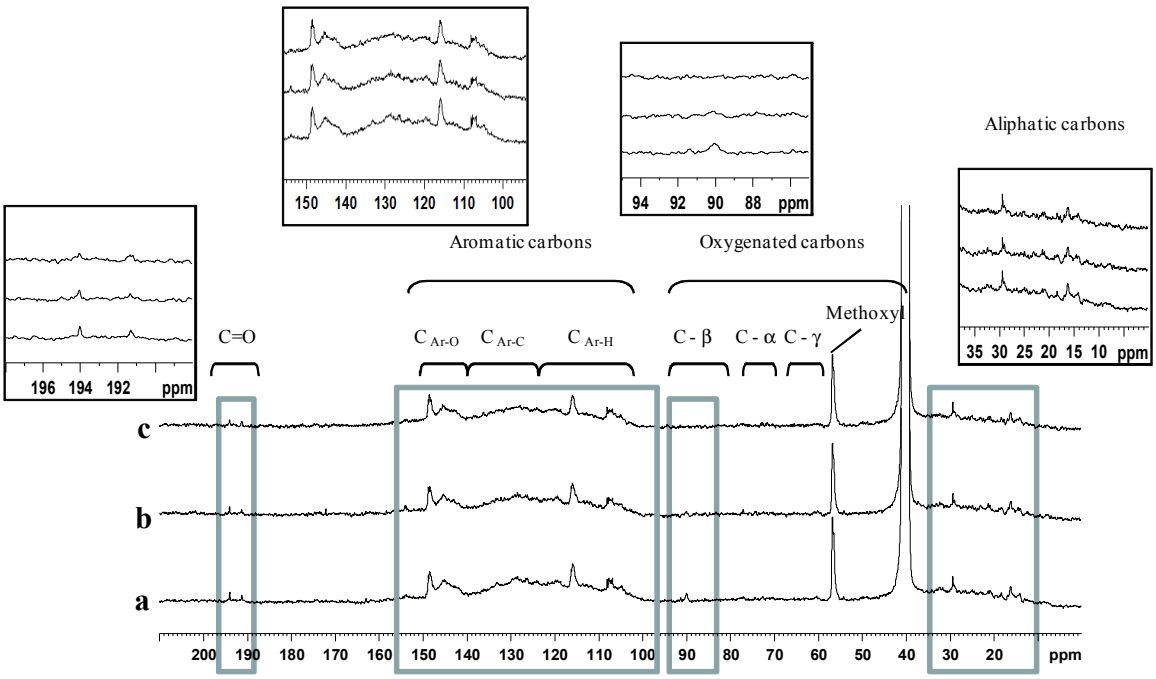

Figure 3.3 ^{13}C NMR spectra of (a) untreated pyrolytic lignin before and (b) after spinning, and (c) pyrolytic lignin treated at 160°C for 1 hour at 30KPa)

Studies into the chemical composition of bio-oil report that more than 5% of the bio-oil are various hydrocarbons and other hydrophobic organic molecules (Walker, 2007) which may, after isolation, remain in the water insoluble fraction of bio-oil (together with pyrolytic lignin). **Figure 3.3** shows the ^{13}C NMR spectra of pyrolytic lignin before (**Figure 3.3a**) and after fibre spinning (**Figure 3.3b**). In addition to the typical lignin aromatic (100-150 ppm), methoxyl (58 ppm) and carbonyl/carboxyl (190-200 ppm)

moieties, there is clear evidence of non-aromatic hydrocarbons (10 to 40 ppm) and oxygenated aliphatic (85-95 ppm) moieties in the pyrolytic lignin.

Table 3.2 Integral of various regions of the ^{13}C NMR of pyrolytic lignin before and after fibre spinning as well as pretreated at 160°C for 1 hour at 30KPa

	Aliphatic Carbons (10-38 ppm)	**Oxygenated Aliphatic Carbons (58-92 ppm)**	**Aromatic Carbons (100-150 ppm)**	**Carbonyl Carbons (170-200 ppm)**
Pyrolytic lignin	5.7	2.1	6.0	2.6
As-spun fibres	4.7	2.0	6.8	2.6
Preheated pyrolytic lignin	3.2	1.9	7.9	2.5

Integrals are based on accurately weighing 105 mg of lignin in 0.5 mL of deuterated DMSO; the integral of aromatic region of untreated pyrolytic lignin were set to 6.0 ppm.

After fibre spinning there is little change in the number of peaks, but the relative intensity, or concentration do change. The corresponding concentration (integrals) of the various chemical moiety regions for the pyrolytic lignin and as-spun pyrolytic lignin fibres are listed in **Table 3.2**. The relative intensity of the various carbon signals associated with the aliphatic (10-38 ppm) and oxygenated moieties (58-92 ppm and 170-200 ppm) has decreased. Of particular significance are those at 90-92 ppm - oxygenated benzyl carbons as well as conjugated β oxygenated carbons; 10-25 ppm - terminal methyl groups attached to methylene, carbonyl (ester) and alkenes; and to a lesser extent, carbons associated with conjugated carbonyl units (e.g. benzaldehyde) at 191.5 and 194 ppm. Thus considering the aforementioned observations in the DTG curves (**Figure 3.2**),

the non-polar hydrocarbons (corresponding to the region 10-38 ppm) are probably the major source of volatile components in pyrolytic lignin. The relative increase in the integral of the aromatic or alkene region (100-150 ppm) after spinning is probably a result of the partial removal of these volatile compounds.

The relative increase in the concentration of aromatic compounds in the pyrolytic lignin upon thermal treatment (fibre spinning/pretreatment) is also evidenced by elemental analysis. As shown in **Table 3.3**, the C/H ratio - an indication of aromaticity, slightly increases after fibre spinning due to the partly removal of the aliphatic hydrocarbons.

Table 3.3 Elemental analysis of pyrolytic lignin before and after fibre spinning as well as pretreated at 160°C for 1 hour at 30KPa

	C/H	C (wt %)	H (wt %)	O (wt %)
Pyrolytic lignin	0.96	67.09	5.87	26.66
As-spun fibres	0.96	67.00	5.85	26.79
Pretreated pyrolytic lignin	1.00	68.34	5.75	25.53

The volatile small molecules typically associated with pyrolytic lignin are probably responsible for another problem encountered in carbon fibre fabrication from pyrolytic lignin. **Figure 3.1(b)** clearly shows that the precursor fibres spun from isolated pyrolytic

lignin cannot be thermostabilized using conditions utilized for other technical lignins (heating rate of 0.5°C/min) (Kadla et al., 2002b; Kubo and Kadla, 2005); the individual fibres that are in contact with each other fuse together even at very low thermostabilization heating rates (0.1°C/min). As mentioned above, the pyrolytic lignin used in this study is in fact the water insoluble fraction of bio-oil, and as such it contains a large number of different hydrocarbons and other hydrophobic organic molecules (Walker, 2007). In addition to their volatility, these small molecules may act as plasticizers (Sperling, 2005), reducing the T_g of the pyrolytic lignin and hence leading to fibre fusing in the thermostabilization process. Unfortunately, due to the chemical changes in lignins during thermostabilization (Braun et al., 2005) we were unable to solubilise the TS fibres and analyze their ^{13}C NMR spectrum.

Despite the good spinning properties of the pyrolytic lignin, a pretreatment to remove volatile components appears necessary to eliminate the large cavity structures in the as-spun fibres, and ensure that the fibres can survive the subsequent thermostabilization process. In the processing of pitch (Morgan, 2005) and other technical lignins (Sudo and Shimizu, 1992; Sudo et al., 1993; Uraki et al., 1995; Kadla et al., 2002b; Kubo and Kadla, 2005; Kubo and Kadla, 2006) to produce carbon fibres certain modifications or treatments prior to fibre spinning are typically performed in order to enhance the materials flowability (Sudo and Shimizu, 1992; Sudo et al., 1993) or spinning property (Uraki et al., 1995). Based on the DTG curve for the (fused) thermostabilized fibres, a large amount of the pyrolytic lignin material can be removed (degraded) by thermally treating the material to temperatures approaching 200 °C.

Therefore, the pyrolytic lignin was subjected to various temperatures ranging from 150°C - 180°C for 0.5 - 6 hrs at a reduced pressure of 30 KPa.

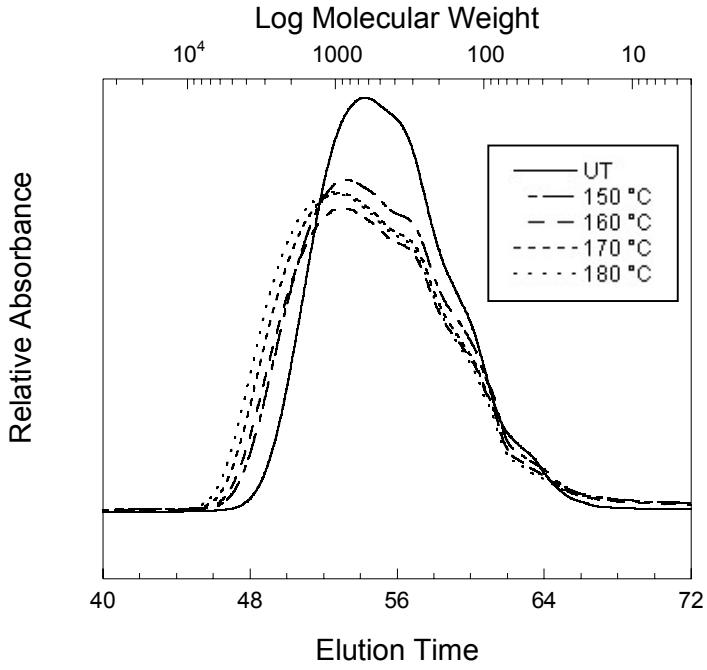

Figure 3.4 GPC traces for untreated pyrolytic lignin (label as UT in the legend) and pyrolytic lignin treated for 1 hr at various temperatures (specified in the legend) at 30KPa

GPC analysis of the pyrolytic lignin and the various lignins obtained after heat treatment confirm the loss of low molecular weight components with increasing time (**Figure 3.4**) and temperature (**Figure 3.5**). Increasing pretreatment temperature from 150 - 180 °C resulted in a significant change in the molecular mass distribution of the pyrolytic lignin (**Figure 3.4**). The mid-to-low molecular mass material seems to decrease significantly at 150 °C accompanied by an increase in higher molecular mass material. This is likely the result of the volatization of low molecular mass components along with some condensation/coupling into larger molecules. Increasing the temperature beyond

150 ^{o}C further leads to an increase in relative molecular mass distribution, albeit the elution profile is quite similar between treatments.

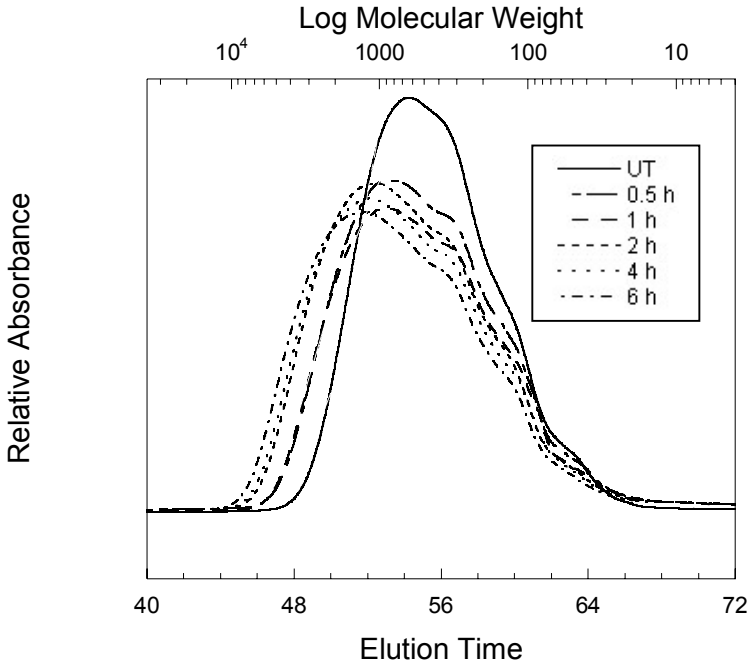

Figure 3.5 GPC traces for untreated pyrolytic lignin (label as UT in the legend) and pyrolytic lignin treated at 160°C for various period of time (specified in the legend) at 30KPa

An almost identical behaviour was observed for increasing the time at temperature. **Figure 3.5** shows the same decrease in mid-to-low molecular mass material with increasing heating time. However, there appears to be a more significant increase in the high molecular mass material region (2000-7000 daltons). In particular, at times of 2 hrs or more the relative average molecular mass distribution contains a significant amount of higher mass material, > 2000 daltons. This is likely due to enhanced condensation reactions between the various pyrolytic components.

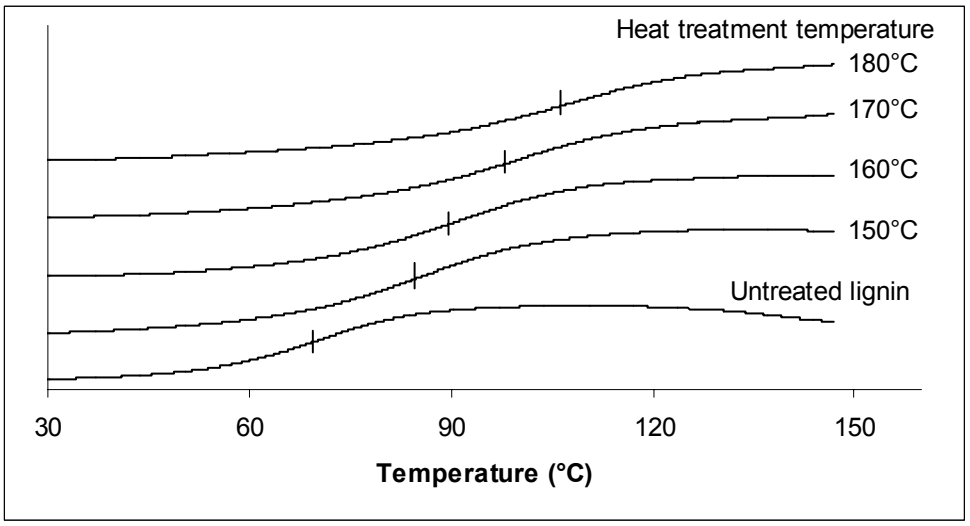

Figure 3.6 DSC thermograms of untreated pyrolytic lignin and pyrolytic lignin treated at various temperatures for 1 hour at 30KPa

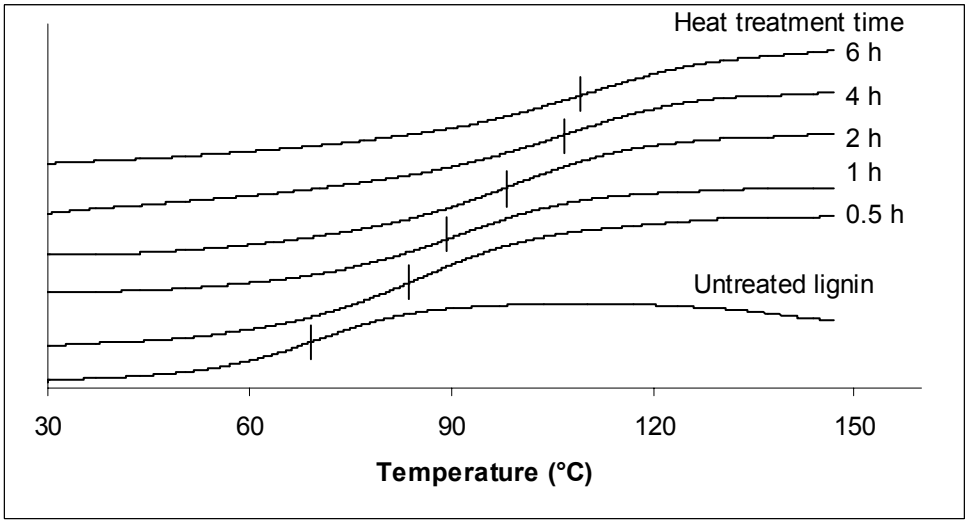

Figure 3.7 DSC thermograms of untreated pyrolytic lignin and pyrolytic lignin treated at 160°C for various period of time at 30KPa

The pretreatment temperature and time have a similar effect on the T_g of the pyrolytic lignin. As shown in **Figure 3.6** and **3.7**, an increase in pretreatment time and temperature both result in an increase in T_g. Again, the increase in T_g can be attributed to

both increasing molecular weight and removal of low molecular mass components, which may have acted as plasticizers.

Table 3.4 Processibility of pyrolytic lignin pretreated under various conditions

Treatment Temperature (°C)	Time of Heat-treatment (hour)				
	0.5	**1**	**2**	**4**	**6**
150	F[a]	F[a]	F[a]	S[b]	S[b]
160	F[a]	S[a]	S[b]	S[b]	NS[c]
170	F[a]	S[a]	S[b]	NS[c]	NS[c]
180	F[b]	NS[c]	NS[c]	NS[c]	NS[c]

F: continuous fibre spinning achieved; fibres fused during TS (0.5°C/min); NS: continuous fibre spinning not possible; S: continuous fibre spinning achieved; fibres survive TS (0.5°C/min); [a] maximum take-up speed ≥ 30 m/min; [b] maximum take-up speed in the range 10-20 m/min; [c] maximum take-up speed < 10 m/min

Based on the above observation from GPC and DSC data, the pretreatment time and temperature have significant influence on the molecular weight, thermal properties and hence processing properties of pyrolytic lignin. The effect of temperature and time of heat treatment on the spinning and thermostabilization properties of pyrolytic lignin are summarized in **Table 3.4**. Increasing the time or temperature of thermal treatment reduced the maximum speed of spinning. High temperature and long pretreatment time dramatically reduced the maximum take-up speeds of the resulting pyrolytic lignin (< 10 m/min) and continuous fibre spinning was not possible for any prolonged period of time

(< 1 min max). As a result, these preparations are considered not spinnable (marked "NS"). At the other extreme, fibres produced from low temperature and short treatment time fused during the thermostabilization process (marked "F"). Only a narrow window of pretreatment conditions is available in which the production of carbon fibre from pyrolytic lignin is possible, labelled "S". It is noted that no experimental design has been performed to optimize the pretreatment conditions in regard to the mechanical properties of the resultant carbon fibres since, in addition to pretreatment time and temperature, there are too many variables in the production process (especially during the spinning process) that significantly affect the mechanical properties of carbon fibres.

The pretreatment conditions of 160°C and 1 hour were chosen to proceed and investigate carbon fibre production due to its better spinning properties. SEM analyses in **Figure 3.1** reveal a clear improvement in fibre morphology with the pretreatment. Compared with the fibres spun from untreated pyrolytic lignin (**Figure 3.1 (a) and 3.1 (b)**), those made from the pretreated pyrolytic lignin (**Figure 3.1 (c) and 3.1 (d)**) appear smooth and continuous with no signs of voids or cavities. Moreover, these fibres could be successfully thermostabilized.

As expected the DTG curve (**Figure 3.2**) of the pretreated pyrolytic lignin also changed, appearing similar to that of the spun untreated pyrolytic lignin but with further reduction in the intensity of the volatile peak (showing less than 3% weight loss). Although not completely removed, as in the DTG curve of thermostabilized untreated pyrolytic lignin, the volatile components of pyrolytic lignin are partly removed after the

heat treatment. The partly removal of these volatiles is sufficient and critical in ensuring fibre integrity during thermostabilization while keeping moderate spinning properties.

Similarly the ^{13}C NMR spectrum (**Figure 3.3c**) of the pretreated pyrolytic lignin revealed changes in the chemical structures present. There is a slight reduction in the methoxyl peak at 57 ppm, likely due to demethoxylation reactions (Braun et al., 2005). Likewise, the peak at around 90 ppm associated with oxygenated aliphatic carbons diminishes completely after the heat-treatment (Braun et al., 2005). Further comparison of the relative integrals for the various regions within the ^{13}C NMR spectra (**Table 3.2**) clearly reveals the extent of changes in the pyrolytic lignin as a result of the heat treatment. The pretreated pyrolytic lignin shows a further decrease in the relative intensity of the carbonyl carbon (170-200 ppm) region, as well as the aliphatic carbon (10-38 ppm) region; again supporting the removal of the volatile components. As with fibre spinning, the aromaticity, as determined by the elemental analysis, C/H (**Table 3.3**) shows a further increase after pretreatment, again corroborating the observations in ^{13}C NMR spectra.

3.1.2 Carbon fibre yield and mechanical properties

Yield is an important aspect of the commercial manufacturing of carbon fibre (Kadla et al., 2002b). Lower yield results in higher production costs per unit weight of product. **Table 3.5** summarizes the yield of each processing stage towards the production of carbon fibres from pyrolytic lignin as well as Alcell and Kraft lignin.

The thermal pretreatment process has a relatively more pronounced effect on the weight loss of the pyrolytic lignin because the Alcell and Kraft lignin are treated for a shorter period of time, optimized for the substrate (Kadla et al., 2002b). As mentioned previously, the purpose of heat-treatment is to remove volatiles from the raw material. Thus another possible reason for the lower pretreatment yield of pyrolytic lignin is that it contains more volatiles than the other two types of lignin, thus requiring a longer pretreatment time. This is also the case for isotropic pitch, which has a significantly lower pretreatment yield of ~40 wt%, attributed to its relatively high temperature pretreatment at more than 350°C.

Table 3.5 Comparison of carbon fibre yields from Alcell, Kraft, and pyrolytic lignin

Lignin Type	Pretreatment (wt%)	Spinning (wt%)	Stabilization (wt%)	Carbonization (wt%)	Overall (wt%)
Kraft	98	98	94	51	46
Alcell	96	99	95	46	42
Pyrolytic Lignin	93	96	95	55	46
Isotropic Pitch[a]	40	95	110	80	33

[a]: Values from literature (Sudo et al., 1993)

For all three types of lignins, there was very little yield losses during fibre spinning (less than 1-4 wt%) and thermostabilization (ca. 4-6 wt%). In contrast commercial

isotropic pitch increases in weight by 10 wt% after thermostabilization as a result of the oxidation conditions (Bahl et al., 1998).

During the carbonization process, most of the non-carbon elements are removed from the precursor fibre (usually more than 90 wt%). Since technical lignins have a carbon content of only 59 wt%-61 wt% (Kadla et al., 2002b), the majority of their weight loss occurred in the carbonization step: pyrolytic-lignin-based fibres 45.0 wt%, loss Kraft lignin ~49 wt% loss and Alcell fibres around ~54 wt%. loss Here the slightly higher carbonization yield of pyrolytic lignin can be attributed to its higher carbon content (~ 67 wt% - **Table 2.2**). In the same way, isotropic pitch only lose ~20 wt% in weight as a result of the higher carbon content - more than 90 wt% (Alcaniz-Monge et al., 2001).

Overall, the total carbon fibre yield from Kraft and pyrolytic lignin were found to be higher than that from Alcell lignin, with pyrolytic lignin having the highest carbon fibre yield of all three at ~ 46 wt%. This is significantly higher than that of isotropic pitch (~33 wt%) (Bahl et al., 1998).

Due to the limitation of the spinning apparatus (inconsistent feeding rate, limited take-up speed and spinneret size), as well as the high solidifying speed of lignin as it exists the spinneret that decreases the ability to stretch the fibres post spinning, the diameters of all three types of lignin carbon fibres are within the range of 30 to 50 μm, which are considerably larger than those of carbon fibres (7 to 14 μm) made from other sources (Sudo et al., 1993; Uraki et al., 1995). Since tensile strength of carbon fibres exhibit significant size dependence: increasing with decreasing fibre diameter (Tagawa

and Miyata, 1997), it is expected that the mechanical properties will further be enhanced by lowering the diameter of pyrolytic lignin fibres, and is an area of current research.

The mechanical properties of the pyrolytic-lignin-based carbon fibres fabricated in this study are comparable, to those made from other technical lignins (Kadla et al., 2002b) (**Table 3.6**). Albeit carbon fibres with moderate mechanical properties can be made from pyrolytic lignin, their mechanical properties are still too weak compared to that of the general performance grade carbon fibres made form isotropic pitch (**Table 3.6**).

Table 3.6 Comparison of mechanical properties of carbon fibres made from Alcell, Kraft, and pyrolytic lignin

Feedstock Material	Diameter (um)	Modulus (GPa)	Strength (MPa)
Kraft Lignin	49 ± 1	41 ± 3	412 ± 39
Alcell Lignin	47 ± 2	37 ± 4	379 ± 34
Pyrolytic Lignin	49 ± 2	36 ± 1	370 ± 38
Isotropic Pitch[a]	8 - 15	40 - 50	600 - 1000

Values are averages of 20 replicates; deviations are 95% confidence interval based on a *T*-statistic;
[a]: Values from literature (Bahl et al., 1998)

3.2 Organoclay reinforced carbon fibre

Using a heat pretreatment step pyrolytic lignin can be used to produce carbon fibres. Although these carbon fibres possess mechanical properties comparable to those of the carbon fibres made from Kraft and Organosolv lignin, their mechanical properties are

inferior to those required for most commercial applications. Since organoclay has been demonstrated to enhance the mechanical properties of most polymer systems (Pavlidou and Papaspyrides, 2008), we have examined the potential of organoclay reinforcement to increase the mechanical properties of pyrolytic lignin-based carbon fibres.

A major concern in the preparation of polymer/clay nano-composites is the achievement of maximum dispersion of the nano-scale clay platelets into the polymer matrix (Goettler et al., 2007). Depending on the degree of dispersion, there are basically two categories of morphology in polymer/clay nano-composites: intercalation, where extended polymer chains occupy the interlayer space between silicate layers, or exfoliation, where the clay platelets are separated apart by at least 10 nm or totally delaminated and randomly dispersed in a continuous polymer matrix (Liu et al., 2006). Typically, the hydrophilic native clay is organically modified to improve its compatibility with the usually hydrophobic polymer matrix. The organically modified clay is thus referred to as organoclay. The modification involves the substitution of the interlayer metallic cations for alkylammonium ions and usually facilitates the intercalation of polymer chains into the clay galleries by increasing their interfacial interactions (Pavlidou and Papaspyrides, 2008). In order to investigate the effect of the interlayer cation/polymer interaction on the dispersion of clay platelets, we chose two types of organoclay (**Table 2.3**) containing the interlayer cations representative of different hydrophobicity. Specifically, Cloisite 20A contains cations with two hydrogenated tallow groups, enabling it to participate in non-bonding interactions with lignin molecules, while the ammonium cations of Cloisite 30B possess both a hydrogenated tallow group and two

hydroxyl ethyl groups which are expected to participate in both non-bonding and hydrogen-bonding interactions with lignin molecules, respectively.

3.2.1 Effect of organoclay on lignin spinning properties

Table 3.7 Spinning properties of pyrolytic lignin with and without organoclay reinforcement

Organoclay Loading (Type)	Spinning Temperature[a] (°C)		Spinning Speed[b] (m/min)
	Zone 1	Zone 2	
0 wt% Organoclay	120	166	36
1 wt% (Cloisite® 20A)	120	168	36
2 wt% (Cloisite® 20A)	120	170	25
5 wt% (Cloisite® 20A)	135	178	18
1 wt% (Cloisite® 30B)	120	162	36
2 wt% (Cloisite® 30B)	125	170	22
5 wt% (Cloisite® 30B)	125	170	18

[a]: Recorded as the rate in which continuous fibre spinning was achieved; [b]: Maximum spinning speed that could be obtained for each sample by adjusting the spinning temperature

The incorporation of organoclay appeared to reduce the spinning properties of pyrolytic lignin; the addition of organoclay increased the temperature required to obtain continuous spinning (**Table 3.7**). This effect became more pronounced for samples with

higher organoclay content (5 wt%), regardless of organoclay type. Likewise, increasing the organoclay content also decreased the fibre spinning rate that could be used to maintain continuous fibre take-up. However, the lignin preparation with the addition of 1 wt% organoclay slightly improved fibre spinning; particularly the Cloisite® 30B organoclay.

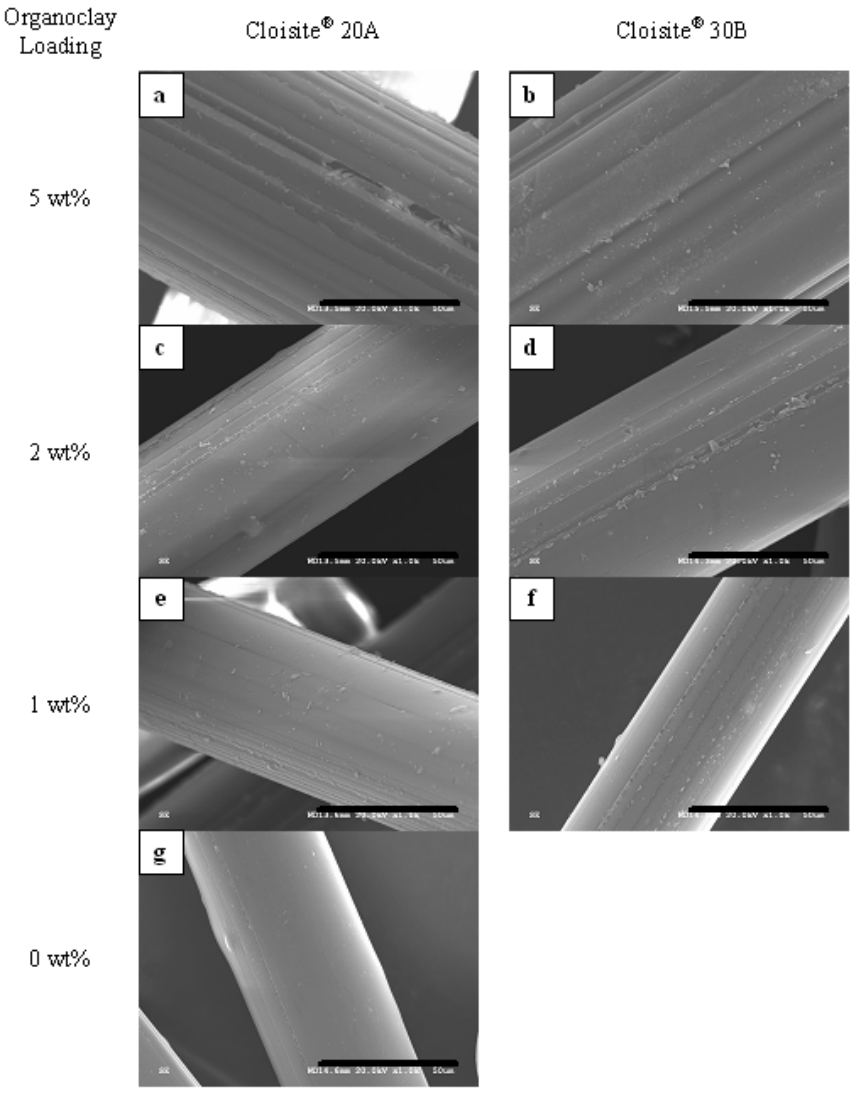

Figure 3.8 SEM micrographs of fibres spun from pyrolytic lignin with and without organoclay reinforcement (For all micrographs, magnification = ×1000, bar = 50μm)

The higher loading of organoclay not only has a negative impact on the spinning properties of the lignin samples, leading to thicker fibres, but also decreased the quality of the as-spun fibres. As illustrated in **Figure 3.8**, the higher the organoclay loading, the rougher the fibre surface. For lignin compounded at 5 wt% organoclay loading, an obvious striated morphology on the fibre surface was observed regardless of organoclay type (**Figure 3.8**). However, the surface roughness itself may not be detrimental to the tensile properties of the resultant carbon fibre, and may in fact enhance the interfacial interaction with the surrounding matrix.

3.2.2 Thermal properties of lignin/organoclay composites

Glass transition temperature (Tg) is the temperature at which polymer materials start to soften and transform from the glassy state to the rubbery state. Above the Tg, some polymer materials are able to flow and spin into fibres (Sperling, 2005). Thermal analysis of the composite powder and corresponding composite fibres reveals the T_g increases with increasing organoclay incorporation (**Table 3.8**). The increase in T_g for the composite powders is consistent with the increase in spinning temperature required for the lignin/organoclay composites with increasing organoclay loadings (**Table 3.7**). After thermal extrusion and fibre spinning, the same trend of increasing T_g with organoclay loading is maintained in the lignin/organoclay composite fibres (**Table 3.8**).

Table 3.8 Glass transition temperatures of lignin/organoclay composites

Organoclay Loading	Composite Powder		Composite Fibre	
	Cloisite® 20A	Cloisite® 30B	Cloisite® 20A	Cloisite® 30B
0 wt%[a]	91	91	96	96
1 wt%	94	94	97	97
2 wt%	94	94	97	97
5 wt%	96	95	101	101

[a]: Pyrolytic lignin without organoclay loading

Table 3.9 Decomposition temperatures of lignin/organoclay composites

Organoclay Loading	Composite Powder		Composite Fibre	
	Cloisite® 20A	Cloisite® 30B	Cloisite® 20A	Cloisite® 30B
0 wt%[a]	235	235	223	223
1 wt%	229	228	217	221
2 wt%	217	229	223	223
5 wt%	198	218	197	210

[a]: Pyrolytic lignin without organoclay loading

Thermal analysis can also provide information regarding the thermal stability of materials. This is typically performed using TGA and measuring the temperature at which 5% weight loss occurs. Generally, the addition of organoclay into the polymer

matrix will enhance thermal stability in that the clay platelets act as a superior insulator and mass transport barrier to the volatile products generated during thermal decomposition (Pavlidou and Papaspyrides, 2008). However, the organoclay reinforced pyrolytic lignin powders and fibres exhibit lower decomposition temperatures than the control lignin (**Table 3.9**). In the composite powders, the decomposition temperatures decrease with increasing organoclay; the extent of decrease being greater for the Cloisite® 20A lignin powders than that of Cloisite® 30B. In the composite fibres, the decrease in decomposition temperatures are less severe, with those of 1-2 wt% appearing to show no change in decomposition temperatures over that of the pure lignin. However, at 5 wt% organoclay, the Cloisite® 20A containing fibres are significantly lower than those using Cloisite® 30B.

3.2.3 Organoclay morphology in as-spun and carbon fibres

Wide-angle X-ray diffraction (WAXD) is commonly performed to estimate the degree of clay dispersion within polymer matrices (Ray and Okamoto, 2003). Based on Bragg's law (Bragg, 1913), this technique allows for the determination of the distances between the adjacent clay platelets. **Figure 3.9** shows the 2θ (diffraction angle) plots obtained from the WAXD of as-spun fibres prepared from lignin/Cloisite® 20A and lignin/Cloisite® 30B composites, respectively.

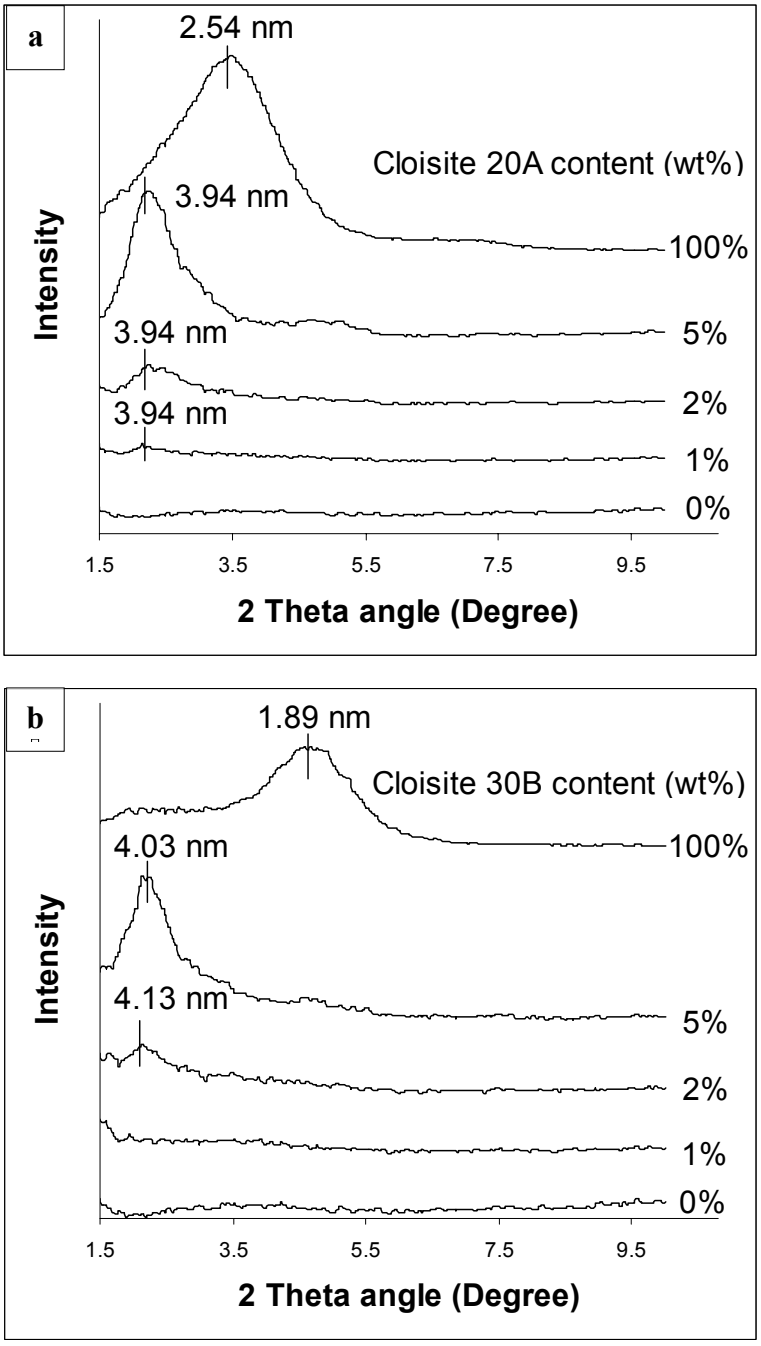

Figure 3.9 Wide-angle X-ray diffractograms of the a) organoclay Cloisite® 20A and as-spun fibres prepared from lignin/Cloisite® 20A composites with organoclay loading 1 wt%, 2 wt%, 5 wt% ; and b) organoclay Cloisite® 30B and as-spun fibres prepared from lignin/Cloisite® 30B composites with organoclay loading 1 wt%, 2 wt%, 5 wt%

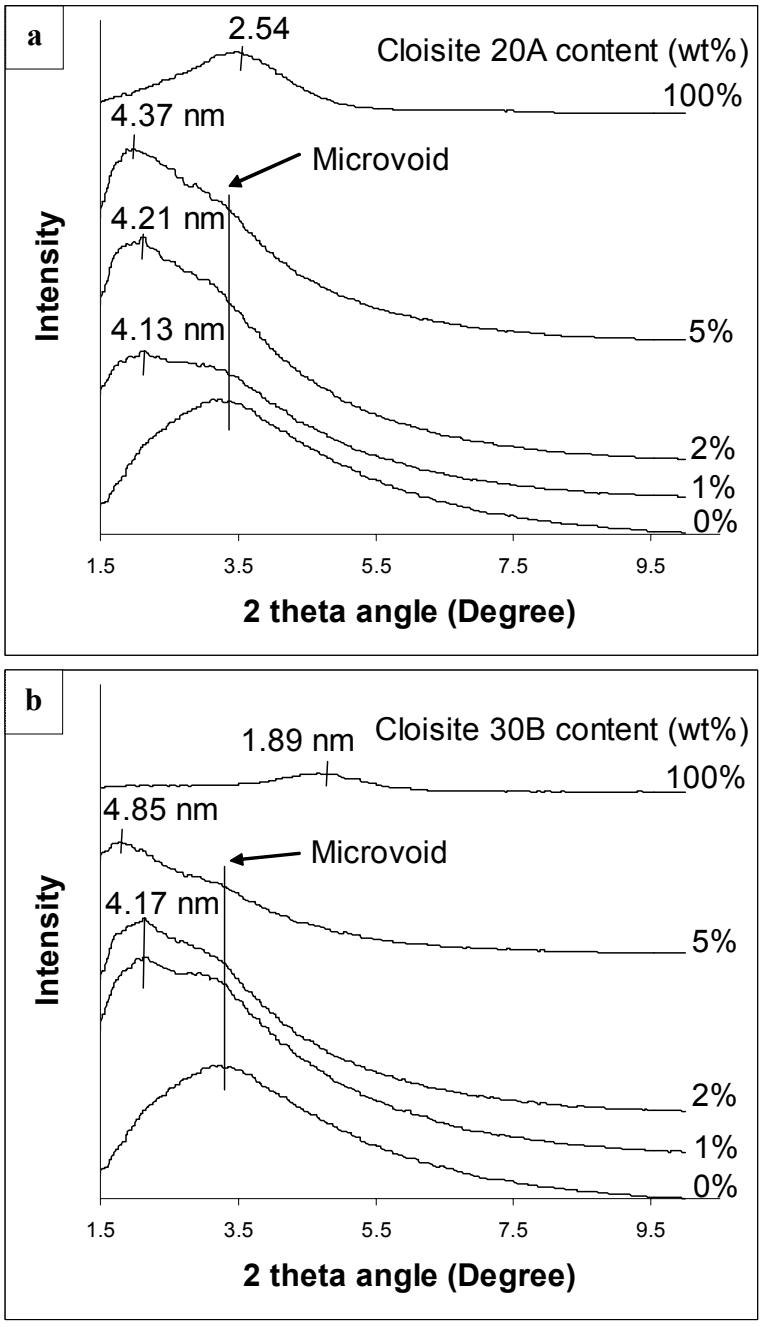

Figure 3.10 Wide-angle X-ray diffractograms (2 theta angle below 10 degree) of the organoclay and carbon fibres prepared from lignin/organoclay composites for a) Cloisite® 20A and b) Cloisite® 30B. Organoclay loadings are 1 wt%, 2 wt%, and 5 wt%

According to Bragg's law the relationship between the 2θ angles and the interlayer spacing of the clay platelets is given by: $\lambda = 2d \sin \theta$, where λ is the wavelength of the X-ray radiation used in the WAXD experiment, d is the distance between the adjacent diffractional lattice planes, and θ is the measured diffraction angle.

Table 3.10 Comparison of d-spacing of clay platelets in the lignin/organoclay composite before and after carbonization (Values were obtained after peak deconvolution)

Organoclay Content	Cloisite® 20A d-spacing (nm)		Cloisite® 30B d-spacing (nm)	
	As-spun Fibre	Carbon Fibre	As-spun Fibre	Carbon Fibre
1 wt%	3.94	4.13	-[a]	4.17
2 wt%	3.94	4.21	4.13	4.17
5 wt%	3.94	4.37	4.03	4.85
100wt%	2.54		1.89	

[a]: No discernable peak for d-spacing determination

For both organoclays, the d-spacing increased substantially after melt compounding (**Table 3.10**), e.g. the peak in the X-ray diffractograms shift to lower 2θ, indicating the successful insertion of lignin molecules into the organoclay galleries. As expected, the chemistry of the organoclay modifier has a discernable effect on the extent of clay intercalation. For lignin reinforced by Cloisite® 20A, the interlayer spacing expanded 55% (2.54 nm to 3.94 nm) regardless of organoclay loading, whereas the d-spacing of the lignin/Cloisite® 30B more than doubled (1.89 nm to 4.03/4.13 nm) for all organoclay

loadings examined in this study. One should also noticed that the d-spacing peak disappear in the fibre with 1% Cloisite® 30B loading. This seems like an indication of exfoliation, but could be a dilution effect.

To facilitate favourable mixing and polymer insertion into clay galleries, native clays are typically modified using organic quaternary ammonium compounds, i.e. organoclays. The organic counterions serve to lower the surface energy between the surface of the organoclay and that of the polymer matrix, thereby facilitating favourable mixing and polymer insertion into the clay galleries (Giannelis, 1996). The two organoclays used in this study were modified from the same native clay and differ only in their counterions (modifier). Cloisite® 20A organoclay has a dimethyl-dihydrogenated tallow ammonium counterion, which is more hydrophobic than the dihydroxyethyl-methyl-tallow ammonium counterion found in Cloisite® 30B (**Table 2.3**). Although pyrolytic lignin, the water insoluble fraction of bio-oil should be considered hydrophobic in regard to water soluble polymers, pyrolytic lignin exhibits a certain degree of polarity owing to its oxygen-containing groups (**Figure 3.3**). Moreover, as it has been shown that technical lignins form strong favourable interaction, e.g. hydrogen-bonding with alcohols and ethers (Kadla and Kubo, 2003), we expect better interaction of lignin with Cloisite® 30B than with Cloisite® 20A. In fact, the higher degree of clay gallery expansion observed for the Cloisite® 30B organoclay may be due to such strong interactions between pyrolytic lignin molecules and the hydroxyethyl moieties of the quaternary ammonium ions.

WAXD analysis (**Figure 3.10**) of the corresponding carbon fibres shows a further expansion of the clay galleries in the Cloisite® 20A composite carbon fibres to more than 4 nm, which increase with increased organoclay loadings. By contrast, the Cloisite® 30B composite carbon fibres do not significantly change from that of the precursor fibres except at the highest organoclay loading (5 wt%) which expands to almost 5 nm in size (**Table 3.10**). It appears that during the manufacturing process of carbon fibres the d-spacing or degree of expansion of the organoclay galleries further increased. The diffractograms of the resultant carbon fibres also show the presence of a broad 2θ angle peak at around 3.3°, ~2.6 nm which can be assigned to microvoids in the carbon fibres (Tomizuka and Johnson, 1978). The microvoids are clearly visible in the 100% lignin carbon fibres, and believed to be responsible for the low tensile strength and modulus of lignin based carbon fibres (Tomizuka and Johnson, 1978). Since this microvoid peak overlaps with the organoclay d-spacing peaks, all diffractograms were deconvoluted prior to determining d-spacing data.

3.2.4 Orientation of organoclay platelets along the fibre axis

In addition to information on d-spacing and the expansion of the organoclay galleries, the X-ray diffraction patterns also provide information regarding the orientation of the organoclay platelets within the fibres. **Figure 3.11** shows the X-ray diffraction patterns of the lignin/organoclay composite as-spun (**Figure 3.11(a)**) and thermostabilized fibres (**Figure 3.11(b)**). The arcs perpendicular to the fibre direction (indicated by the thick arrows) in the diffraction pattern is an indication of organoclay orientation along the fibre axis.

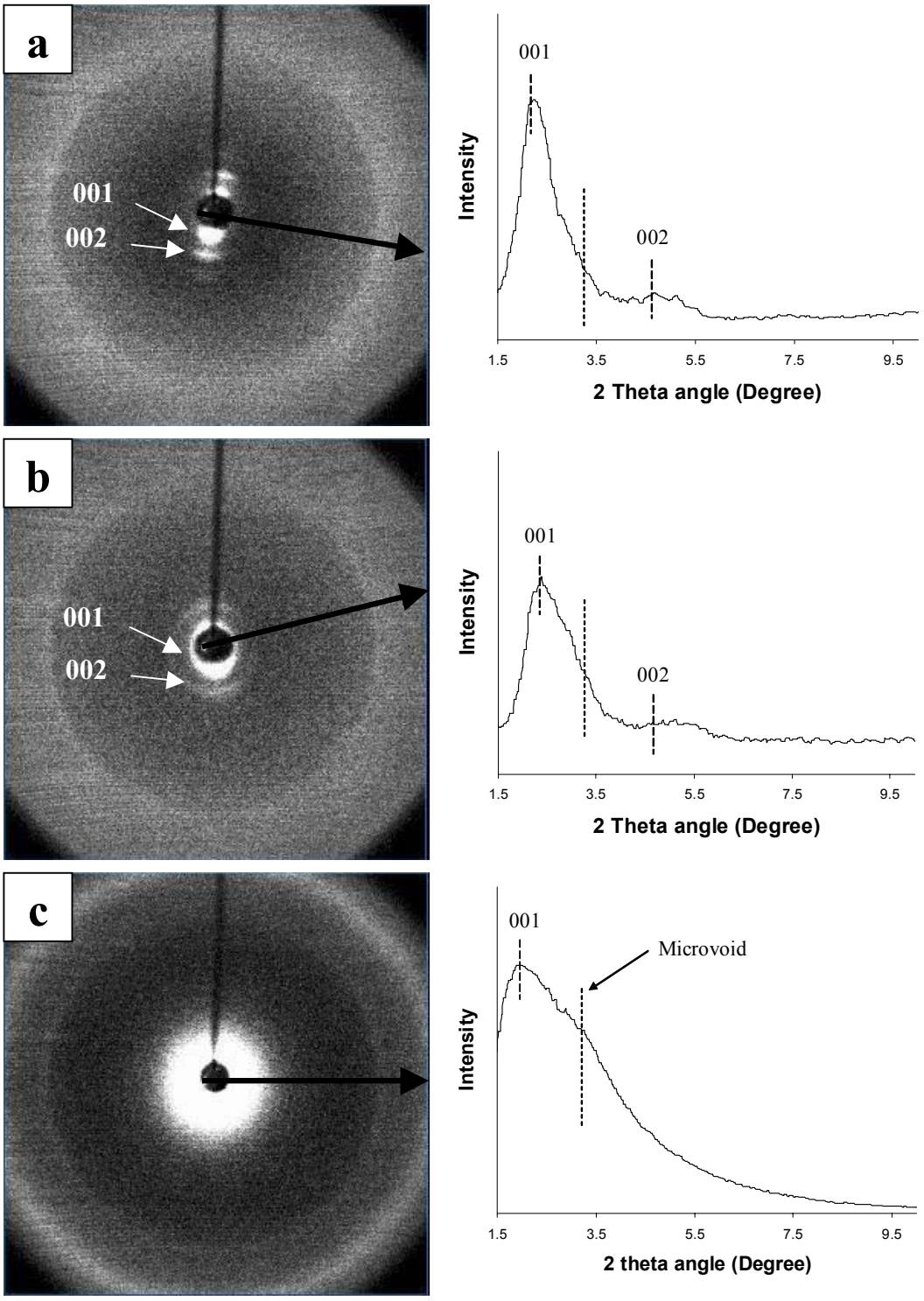

Figure 3.11 Wide-angle X-ray diffraction patterns of the fibre samples with 5% Cloisite® 20A organoclay loading; (a) as-spun fibre; (b) thermostabilized fibre and (c) carbon fibre. The black arrow in each pattern indicates the fibre direction during measurement

The orientation is likely created during the fibre spinning process due to hot stretching and is believed to contribute positively to the tensile properties along the fibre axis. Comparison of the WAXD patterns for the as-spun, thermostabilized and carbon fibres reveals the sharp band pattern associated with the organoclay orientation decreases with increasing thermal treatment. WAXD pattern associated with the carbon fibres appear to have no preferred clay platelet orientation, as demonstrated by the bright ring in the diffraction pattern (**Figure 3.11(c)**). However, this loss of orientation, or introduction of randomness may be a result of the increasing microvoids that are being generated and overlap this region of the diffractogram (**Figure 3.10**). In fact the 2θ plot of the WAXD pattern for thermostabilized fibre do not give discernable evidence of microvoid formation at around 3.3°, but a more randomly distributed 001 and 002 reflection pattern can be found in the corresponding WAXD diffractogram (**Figure 3.11(b)**). Thus it is more likely that the orientation is disrupted in the thermostabilization (fibres under tension) and carbonization process during which tension was not applied to the fibres.

3.2.5 Enhancement of graphitic crystalline perfection by organoclay

The tensile properties of carbon fibres rely heavily on the 3-dimensional perfection of their crystalline structure (Johnson, 1987). The inter-planar spacing (d_{002}) is an indication of the degree of alignment of the graphene planes within the graphitic structure. The theoretical value of this inter-planar spacing for an ideal graphite crystal is 0.3354 nm (Pierson, 1993). But for commercial carbon fibres, this value usually ranges from more than 0.3440 for PAN-based carbon fibres to around 0.3400 for those based on pitch (Pierson, 1993).

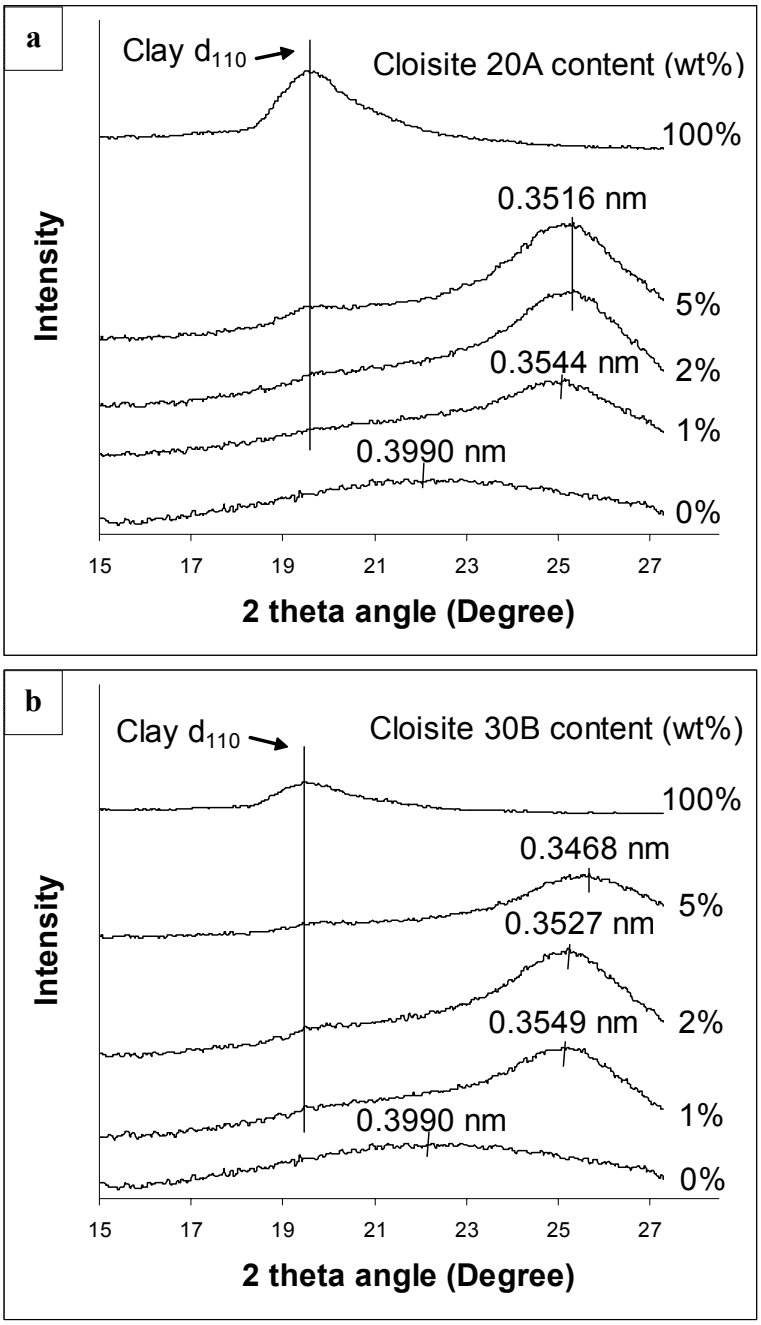

Figure 3.12 Wide-angle X-ray diffractograms (2 theta angle above 10) of the organoclay and carbon fibres prepared from lignin/organoclay composites for a) Cloisite® 20A and b) Cloisite® 30B. Organoclay loadings are 1 wt%, 2 wt%, and 5 wt%

As the d_{002} of lattice plane decreases and approaches the theoretical value of 0.3354 nm, the turbostratic structure of the carbon fibres gets closer to the ideal structure of graphite. Generally, the shorter the inter-layer spacing (d_{002} spacing) of the graphene planes perpendicular to the fibre axis, the higher the tensile strength and modulus of the carbon fibres (Johnson, 1987). **Figure 3.12** shows the 2θ plot for the various composite carbon fibres and the corresponding inter-planar spacing. The pyrolyitc-lignin-based carbon fibres exhibit a broad peak at ~22° in the diffractogram (**Figure 3.12**), indicating a broad inter-planar spacing (d_{002}) distribution centered at ~0.3990 nm, significantly higher than that of ideal graphite crystal and commercial carbon fibres.

Table 3.11 The inter-layer spacing (in nanometres) of graphitic structure in the carbon fibres made from lignin/organoclay composite

Organoclay Loading	Organoclay Type[b]	
	Cloisite® 20A (nm)	Cloisite® 30B (nm)
0 wt%[a]	0.3990 ± 0.0609	0.3990 ± 0.0609
1 wt%	0.3544 ± 0.0086	0.3549 ± 0.0106
2 wt%	0.3516 ± 0.0110	0.3527 ± 0.0121
5 wt%	0.3516 ± 0.0110	0.3468 ± 0.0079

[a]: Pyrolytic lignin without organoclay loading; [b]: ± values calculated from full width half maximum of the respective peak; theoretical inter-layer spacing of graphite: 0.3354 nm

Organoclays have been reported to facilitate graphitization and assist in developing highly ordered graphite crystals for a number of polymer precursors (Kyotani et al., 1988;

Sonobe et al., 1988a; Sonobe et al., 1988b; Sonobe et al., 1990; Sonobe et al., 1991). In this study, we also observed this catalytic effect in the diffractograms of carbon fibres made from lignin/organoclay composites.

In **Figure 3.12**, both types of organoclay gave a sharper peak above 25° 2θ regardless of organoclay content. The corresponding inter-layer spacing (d_{002}) values were calculated and are listed in **Table 3.11**. All of the carbon fibres with organoclay loadings exhibit a shorter d_{002} and sharper signals (indicated by the full width half maximum of the peak in **Table 3.11**), thus resulting in a more ordered structure. A general trend of increasing structure perfection with organoclay loading was observed for carbon fibres containing both types of organoclay.

3.2.6 Mechanical properties and yield

The addition of organoclay did not significantly affect the mechanical properties of the pyrolytic lignin fibres (**Table 3.12**). For both organoclays, the maximum tensile strength and Young's modulus were observed for the 1 wt% organoclay loadings. The Cloisite® 20A fibres showed a 10% and 17% increase in mean tensile strength and modulus as oppose to 33% and 22%, respectively for Cloisite® 30B; increasing the addition of organoclay decreases the mechanical properties. However, fibre diameter increased with organoclay loading for both organoclays. Since tensile strength is negatively affected by increasing fibre diameter (Tagawa and Miyata, 1997), the lower strength of the fibres with higher organoclay loading may be partially attributable to their larger fibre diameters (**Table 3.12**).

Table 3.12 Tensile properties of as-spun fibres with and without organoclay reinforcement

Organoclay Loading (Type)	Diameter (um)	Young's Modulus (GPa)	Tensile Strength (MPa)
0 wt% Organoclay	51 ± 4	4.9 ± 0.5	23 ± 3
1 wt% (Cloisite® 20A)	51 ± 1	5.4[a] ± 0.3	27[a] ± 3
2 wt% (Cloisite® 20A)	70 ± 4	5.3[a] ± 0.3	23[a] ± 2
5 wt% (Cloisite® 20A)	74 ± 6	4.4[a] ± 0.4	17[b] ± 3
1 wt% (Cloisite® 30B)	47 ± 2	6.5[b] ± 0.5	28[b] ± 2
2 wt% (Cloisite® 30B)	71 ± 3	5.3[a] ± 0.2	26[a] ± 2
5 wt% (Cloisite® 30B)	76 ± 4	5.3[a] ± 0.3	17[b] ± 2

Values are averages of 20 replicates; deviations are 95% confidence interval based on a *T*-statistic;
[a]: values are not significantly different from those without organoclay loading; [b]: values are significantly different from those without organoclay loading

To determine if there were differences in mean tensile strength and modulus values between the lignin fibres with and without organoclay reinforcement an analysis of variance (ANOVA) was performed. From the ANOVA results it appears that only the 1 wt% Cloisite® 30B lignin fibres show a significant increase in tensile strength and modulus as compared to the pure lignin fibres. As well, for both organoclays the higher loadings (5 wt%) significantly decreased tensile strength's but did not impact modulus;

however, in both cases the fibre diameters were significantly larger than the pure lignin control fibres.

Table 3.13 Tensile properties of carbon fibres with and without organoclay reinforcement

Organoclay Loading (Type)	Diameter (um)	Young's Modulus (GPa)	Tensile Strength (MPa)
0% Clay	49 ± 2	36 ± 1	370 ± 38
1% (Cloisite® 20A)	45 ± 1	32[b] ± 1	422[b] ± 24
2% (Cloisite® 20A)	50 ± 2	29[b] ± 1	307[b] ± 25
5% (Cloisite® 20A)	55 ± 2	26[b] ± 1	240[b] ± 17
1% (Cloisite® 30B)	47 ± 1	32[b] ± 1	438[b] ± 24
2% (Cloisite® 30B)	50 ± 1	30[b] ± 1	357[a] ± 29
5% (Cloisite® 30B)	57 ± 2	30[b] ± 1	255[b] ± 25

Values are averages of 20 replicates; deviations are 95% confidence interval based on a *T*-statistic;
[a]: values are not significantly different from those without organoclay loading; [b]: values are significantly different from those without organoclay loading

A similar trend in tensile strength is obtained for the corresponding carbon fibres (**Table 3.13**). Again, the 1 wt% Cloisite® 30B organoclay loading fibres have the highest tensile strength, but so too were the 1 wt% Cloisite® 20A carbon fibres significantly stronger in tensile strength than the pure lignin fibres. In both organoclay systems, tensile

strength decreases with increasing organoclay loading. Unlike the precursor fibres, the carbon fibre modulus values dropped slightly upon incorporation of organoclay, and decreased with increasing organoclay content. This might be attributable to: i) the loss of preferred orientation of the clay platelets along the fibre axis; and ii) the presence of microvoids within the carbon fibre.

Another important aspect of the commercial manufacturing of carbon fibre is carbon fibre yield; lower yield results in higher production costs per unit weight of the product. Regardless of organoclay type and loading, the addition of organoclay slightly changed the overall yield of carbon fibre production, from 45 wt% for samples without organoclay loading, to 46 – 47 wt% for samples with organoclay regardless of the organoclay loading.

4 CONCLUSION

4.1 Carbon fibre preparation

In the process of carbon fibre preparation, we employed procedures and conditions similar to those used in the fabrication of carbon fibres based on Kraft and Alcell lignin (Kadla et al., 2002b; Kubo and Kadla, 2005). It was found that the pretreatment is a critical step in the successful preparation of carbon fibres from pyrolytic lignin. The untreated pyrolytic lignin tended to develop hollow structures in the process of spinning and the spun fibres fuse together during thermostabilization. Although the hollow fibre structure may be an advantage in applications where high surface area is required, it will reduce the strength of the resultant carbon fibres. In fact, fibre fusing during the thermostabilization process may be the biggest concern in making carbon fibre from untreated pyrolytic lignin. These disadvantages of pyrolytic lignin were effectively eliminated by pretreatment at elevated temperatures under reduced pressure. The temperature and time of pretreatment had strong effects on the carbon fibre production. Higher temperature and longer time led to poor fibre spinning of pyrolytic lignin, whereas lower temperature and shorter time resulted in lignin fibres fusing together in the subsequent thermostabilization process. Only a narrow window between these two extremes was found to be suitable for carbon fibre production. Within this window the pretreatment condition that gives the best spinning properties was found to be 160°C for 1 hour at 30 kPa reduced pressure. The pyrolytic lignin treated under this condition produced carbon fibres with mechanical properties and yield comparable to those based on Kraft and Alcell lignin; however, too weak for commercial applications.

4.2 Organoclay reinforced carbon fibre

The tensile strength of pyrolytic lignin based carbon fibres was improved (12%) by organoclay reinforcement at loadings below 2 wt%. Wide-angle X-ray diffraction analysis of the resulting composite as-spun fibres revealed the successful intercalation of the organoclay within the pyrolytic lignin matrix. Intercalation was achieved for both types of organoclays used in this study, with Cloisite® 30B showing better dispersion (d-spacing increased by 55%) in the pyrolytic lignin matrix as compared with Cloisite® 20A (d-spacing increased by 113-119%). The intercalation was maintained after the composite fibres were made into carbon fibres. The incorporated organoclay also served as a catalyst during carbonization. Wide-angle X-ray diffraction revealed an improvement in the graphitic structure upon incorporation of both types of organoclay, and the degree of structure perfection increased with organoclay loading.

Increasing the organoclay content above 1 wt% resulted in a drop in tensile strength of both as-spun and carbon fibres. This may be related to fibre diameter which is known to decrease with increasing fibre diameters; the addition of organoclay to the pyrolytic lignin led to poor fibre spinning, which increased with organoclay loading and gave rise to thicker fibres.

By contrast, only the 1 wt% Cloisite® 30B as-spun fibres showed an increase in Young's modulus (increased to 6.5 GPa from 4.9 GPa for the neat lignin fibre). For all other as-spun fibres there was no change in Young's modulus, while all of the carbon fibres dropped (by 16-38%) upon addition of both types of organoclays and decreased as

organoclay content increased. This might be attributable to the presence of microvoids in the carbon fibre as well as the lack of preferred orientation of clay platelets along the fibre axis.

Although the addition of organoclay to pyrolytic lignin can improve mechanical properties of the lignin-based fibres. Compared with commercial general performance carbon fibres (tensile strength: 1 GPa; modulus: 50 GPa), the organoclay reinforced carbon fibres based on pyrolytic lignin (with 1% loading of Cloisite 30B) are too weak (tensile strength: 438 MPa; modulus: 32 GPa) for commercial application.

4.3 Comments and future work

This work demonstrated the possibility of preparing carbon fibres from pyrolytic lignin. Although the mechanical properties and yield of pyrolytic lignin-based carbon fibres are found to be comparable to those of the carbon fibres based on Kraft and Alcell lignin, they are still too weak for commercial applications. The proposed method of organoclay reinforcement for carbon fibres in this study only improved the tensile strength to a limited extent with modulus dropped slightly. There are several reasons for this ineffective reinforcement. First, the moderate dispersion of clay platelets is a source of inclusions and flaws that generate microvoids (Johnson et al., 1975). These defects facilitate crack formation and propagation during tensile test, thus directly reduce the tensile strength. Another reason for the moderate tensile strength of the reinforced carbon fibre might be the lack of bonding or affinity between the silicate layer and the carbon matrix, the fact of which will also decrease the tensile modulus of the carbon fibre.

Finally, the large diameter of the carbon fibre also lowers the tensile strength and modulus.

The recommended future work will be mainly based on the above three points. In order to further increase the degree of clay platelet dispersion in the precursor, one can optimize the melt compounding conditions (Dennis et al., 2001), including the screw design, mean residence time and shear intensity in the extruder etc.

Since a trend of increase in tensile strength with organoclay loading below 2 wt% was observed, a possible extension of this thesis could be to zoom in this range and find the critical organoclay content that gives the highest tensile strength.

Other characterization techniques (transmitting electron microscope and rheology analysis) can be used to investigate the clay dispersion within lignin matrix.

Further, it is also recommended that the carbonization temperature be increased to form silicon carbide which will dramatically increase the bonding between the reinforcement and the matrix.

On the other hand, carbon nanotube may be used instead of organoclay as the nano-reinforcement in order to achieve better affinity between reinforcing agent and carbon matrix as well as reducing the microvoids which are probably generated by the organoclay.

Finally, one is also able to reduce the fibre diameter by electrospinning that gives fibres with size in the nanometre scale. As tensile strength is correlated to fibre diameter, the production of micron-to-submicron diameter fibres may further enhance the molecular orientation of lignin within the fibres and lead to enhance tensile strength.

REFERENCES

Adler, E. (1977). "Lignin Chemistry - Past, Present and Future." Wood Science and Technology **11**(3): 169-218.

Alcaniz-Monge, J., D. Cazorla-Amoros, et al. (2001). "Characterisation of coal tar pitches by thermal analysis, infrared spectroscopy and solvent fractionation." Fuel **80**(1): 41-48.

Alexandre, M. and P. Dubois (2000). "Polymer-layered silicate nanocomposites: preparation, properties and uses of a new class of materials." Materials Science & Engineering R-Reports **28**(1-2): 1-63.

Bahl, O. P., Z. Shen, et al. (1998). Manufacture of Carbon Fibers. Carbon Fibers. J. B. Donnet, T. K. Wang, J. C. M. Peng and S. Rebouillat. New York, Marcel Dekker**:** 1-84.

Bayerbach, R. and D. Meier (2009). "Characterization of the water-insoluble fraction from fast pyrolysis liquids (pyrolytic lignin). Part IV: Structure elucidation of oligomeric molecules." Journal of Analytical and Applied Pyrolysis **85**(1-2): 98-107.

Bayerbach, R., V. D. Nguyen, et al. (2006). "Characterization of the water-insoluble fraction from fast pyrolysis liquids (pyrolytic lignin) - Part III. Molar mass characteristics by SEC, MALDI-TOF-MS, LDI-TOF-MS, and Py-FIMS." Journal of Analytical and Applied Pyrolysis **77**(2): 95-101.

Bennett, N. M., S. S. Helle, et al. (2009). "Extraction and hydrolysis of levoglucosan from pyrolysis oil." Bioresource Technology **100**(23): 6059-6063.

Boerjan, W., J. Ralph, et al. (2003). "Lignin biosynthesis." Annual Review of Plant Biology **54**: 519-546.

Bragg, W. H. (1913). "The structure of the diamond." Proceedings of the Royal Society of London Series a-Containing Papers of a Mathematical and Physical Character **89**(610): 277-291.

Braun, J. L., K. M. Holtman, et al. (2005). "Lignin-based carbon fibers: Oxidative thermostabilization of kraft lignin." Carbon **43**(2): 385-394.

Brown, R. C. (2006). Biomass Refineries Based on Hybrid Thermochemical-Biological Processing - An Overview. Biorefineries - Industrial Processes and Products. B. Kamm, P. R. Gruber and M. Kamm. Weinheim, Wiley-VCH Verlag. **1:** 227-252.

Brydson, J. A. (1999). Plastics Materials. Oxford, Butterworth-Heinemann.

Capanema, E. A., M. Y. Balakshin, et al. (2004). "A comprehensive approach for quantitative lignin characterization by NMR spectroscopy." Journal of Agricultural and Food Chemistry **52**(7): 1850-1860.

Capanema, E. A., M. Y. Balakshin, et al. (2005). "Quantitative characterization of a hardwood milled wood lignin by nuclear magnetic resonance spectroscopy." Journal of Agricultural and Food Chemistry **53**(25): 9639-9649.

Carter, L. W., J. G. Hendricks, et al. (1950). Elastomer reinforced with a modified clay. United States, National Lead Co.

Chang, H. M., E. B. Cowling, et al. (1975). "Comparative Studies on Cellulolytic Enzyme Lignin and Milled Wood Lignin of Sweetgum and Spruce." Holzforschung **29**(5): 153-159.

Chen, J. C. and I. R. Harrison (2002). "Modification of polyacrylonitrile (PAN) carbon fiber precursor via post-spinning plasticization and stretching in dimethyl formamide (DMF)." Carbon **40**(1): 25-45.

Compere, A. L., W. L. Griffith, et al. (2001). "Low cost carbon fiber from renewable resources." Advancing Affordable Materials Technology **33**: 1306-1314.

Dennis, H. R., D. L. Hunter, et al. (2001). "Effect of melt processing conditions on the extent of exfoliation in organoclay-based nanocomposites." Polymer **42**(23): 9513-9522.

Diefendorf, R. J. and D. M. Riggs (1980). Forming optically anisotropic pitches. United States, Exxon Research & Engineering Co.

Dynamotive Website, http://www.dynamotive.com.

Edie, D. D. (1990). Pitch and Mesophase Fibers. Carbon Fibers Filaments and Composites. J. L. Figueiredo, C. A. Bernardo, R. T. K. Baker and K. J. Huttinger. Dordrecht / Boston / London, Kluwer Academic Publishers.

Fitzer, E. (1990). Carbon Fibres - Present State and Future Expectations. Carbon Fibers Filaments and Composites. J. L. Figueiredo, C. A. Bernardo, R. T. K. Baker and K. J. Huttinger. Dordrecht / Boston / London, Kluwer Academic Publishers**:** 3-41.

Fitzer, E. and D. J. Muller (1975). "Influence of Oxygen on Chemical-Reactions During Stabilization of Pan as Carbon-Fiber Precursor." Carbon **13**(1): 63-69.

Fratini, E., M. Bonini, et al. (2006). "SANS analysis of the microstructural evolution during the aging of pyrolysis oils from biomass." Langmuir **22**(1): 306-312.

Fujiwara, S. and T. Sakamoto (1976). Method for manufacturing a clay-polyamide composite. Japan, Unitika K. K.

Fukuoka, Y. (1969). "Carbon fiber made form lignin." Japan Chemical Quarterly **5**(3): 63-66.

Gargulak, J. D. and S. E. Lebo (2000). Commercial Use of Lignin-Based Materials. Lignin: Historical, Biological, and Materials Perspectives. W. G. Glasser, R. A. Northey and T. P. Schultz. Washington D.C., American Chemical Society**:** 304-320.

Giannelis, E. P. (1996). "Polymer layered silicate nanocomposites." Advanced Materials **8**(1): 29-&.

Giannelis, E. P. (1998). "Polymer-layered silicate nanocomposites: Synthesis, properties and applications." Applied Organometallic Chemistry **12**(10-11): 675-680.

Gilman, J. W. (1999). "Flammability and thermal stability studies of polymer layered-silicate (clay) nanocomposites." Applied Clay Science **15**(1-2): 31-49.

Glasser, W. G., C. A. Barnett, et al. (1983). "The Chemistry of Several Novel Bioconversion Lignins." Journal of Agricultural and Food Chemistry **31**(5): 921-930.

Glasser, W. G., R. A. Northey, et al. (2000). Lignin: Historical, Biological, and Materials Perspectives. Washington DC, ACS.

Goettler, L. A., K. Y. Lee, et al. (2007). "Layered silicate reinforced polymer nanocomposites: Development and applications." Polymer Reviews **47**(2): 291-317.

Gosselink, R. J. A., A. Abacherli, et al. (2004). "Analytical protocols for characterisation of sulphur-free lignin." Industrial Crops and Products **19**(3): 271-281.

Gu, A. J. and F. C. Chang (2001). "A novel preparation of polyimide/clay hybrid films with low coefficient of thermal expansion." Journal of Applied Polymer Science **79**(2): 289-294.

Higuchi, T. (1985). Biosynthesis of Lignin. New York, Academic Press.

Holtman, K. M., H. M. Chang, et al. (2003). "Elucidation of lignin structure through degradative methods: Comparison of modified DFRC and thioacidolysis." Journal of Agricultural and Food Chemistry **51**(12): 3535-3540.

Holtman, K. M., H. M. Chang, et al. (2007). "An NMR comparison of the whole lignin from milled wood, MWL, and REL dissolved by the DMSO/NMI procedure." Journal of Wood Chemistry and Technology **27**(3-4): 179-200.

Huang, J. C., Z. K. Zhu, et al. (2001). "Poly(etherimide)/montmorillonite nanocomposites prepared by melt intercalation: morphology, solvent resistance properties and thermal properties." Polymer **42**(3): 873-877.

Jiang, X. X. and N. Ellis (2010). "Upgrading Bio-oil through Emulsification with Biodiesel: Mixture Production." Energy & Fuels **24**(2): 1358-1364.

John, M. J. and S. Thomas (2008). "Biofibres and biocomposites." Carbohydrate Polymers **71**(3): 343-364.

Johnson, D. J. (1987). "Structure property relationships in carbon-fibers." Journal of Physics D-Applied Physics **20**(3): 286-291.

Johnson, D. J., I. Tomizuka, et al. (1975). "Fine-Structure of Lignin-Based Carbon-Fibers." Carbon **13**(4): 321-325.

Kadla, J. F. and Q. Dai (2006). Pulp. Kirk-Othmer Encyclopedia of Chemical Technology. Hoboken, Wiley-Interscience. **21:** 1-47.

Kadla, J. F. and S. Kubo (2003). "Miscibility and hydrogen bonding in blends of poly(ethylene oxide) and kraft lignin." Macromolecules **36**(20): 7803-7811.

Kadla, J. F., S. Kubo, et al. (2002a). "Novel hollow core fibers prepared from lignin polypropylene blends." Journal of Applied Polymer Science **85**(6): 1353-1355.

Kadla, J. F., S. Kubo, et al. (2002b). "Lignin-based carbon fibers for composite fiber applications." Carbon **40**(15): 2913-2920.

Kawasumi, M., M. Kohzaki, et al. (1989). Process for producing composite material. United States, Kabushiki Kaisha Toyota Chuo Kenkyusho (Aichi, JP).

Kojima, Y., A. Usuki, et al. (1993). "Mechanical-Properties of Nylon 6-Clay Hybrid." Journal of Materials Research **8**(5): 1185-1189.

Kringstad, K. P. and R. Morck (1983). "C-13-NMR Spectra of Kraft Lignins." Holzforschung **37**(5): 237-244.

Kubo, S., N. Ishikawa, et al. (1997). "Preparation of lignin fibers from softwood acetic acid lignin - Relationship between fusibility and the chemical structure of lignin." Mokuzai Gakkaishi **43**(8): 655-662.

Kubo, S. and J. F. Kadla (2004). "Poly(ethylene oxide)/organosolv lignin blends: Relationship between thermal properties, chemical structure, and blend behavior." Macromolecules **37**(18): 6904-6911.

Kubo, S. and J. F. Kadla (2005). "Lignin-based carbon fibers: Effect of synthetic polymer blending on fiber properties." Journal of Polymers and the Environment **13**(2): 97-105.

Kubo, S. and J. F. Kadla (2006). Carbon Fibers from Lignin-Recyclable Plastic Blends. Encyclopedia of Chemical Processing. S. Lee. New York, Taylor & Francis. **1:** 317-331.

Kubo, S., Y. Uraki, et al. (1998). "Preparation of carbon fibers from softwood lignin by atmospheric acetic acid pulping." Carbon **36**(7-8): 1119-1124.

Kubo, S., T. Yoshida, et al. (2007). "Surface porosity of lignin/PP blend carbon fibers." Journal of Wood Chemistry and Technology **27**(3-4): 257-271.

Kyotani, T., N. Sonobe, et al. (1988). "Formation of highly orientated graphite from polyacrylonitrile by using a two-dimensional space between montmorillonite lamellae." Nature **331**(6154): 331-333.

Larrain, R., L. H. Tagle, et al. (1981). "Glass-Transition Temperaturemolecular Weight Relation for Poly(Hexamethylene Perchloroterephthalamide)." Polymer Bulletin **4**(8): 487-490.

LeBaron, P. C., Z. Wang, et al. (1999). "Polymer-layered silicate nanocomposites: an overview." Applied Clay Science **15**(1-2): 11-29.

Lebo, S. E., J. D. Gargulak, et al. (2004). Lignin. Encyclopedia of Polymer Science and Technology. H. F. Mark. Hoboken, John Wiley & Sons, Inc. **3:** 100-124.

Lebo, S. E., J. D. Gargulak, et al. (2007). Lignin. Kirk-Othmer Encyclopedia of Chemical Technology. A. Seidel. Hoboken, John Wiley & Sons, Inc. **15:** 1-32.

Lee, D. C. and L. W. Jang (1998). "Characterization of epoxy-clay hybrid composite prepared by emulsion polymerization." Journal of Applied Polymer Science **68**(12): 1997-2005.

Lisicki, Z., W. Majewski, et al. (1988). "Coal-Tar Purification, Distribution and Characterization by Supercritical Extraction." Fuel Processing Technology **20**(1-3): 103-121.

Liu, J., W. J. Boo, et al. (2006). "Intercalation and exfoliation: A review on morphology of polymer nanocomposites reinforced by inorganic layer structures." Materials and Manufacturing Processes **21**(2): 143-151.

Liu, L. M., Z. N. Qi, et al. (1999). "Studies on nylon 6 clay nanocomposites by melt-intercalation process." Journal of Applied Polymer Science **71**(7): 1133-1138.

Lora, J. H. and W. G. Glasser (2002). "Recent industrial applications of lignin: A sustainable alternative to nonrenewable materials." Journal of Polymers and the Environment **10**(1-2): 39-48.

Mansmann, M., G. Winter, et al. (1973). Process for the production of carbon fibers. United States, Bayer Aktiengesellschaft.

Marchessault, R. H., S. Coulombe, et al. (1982). "Characterization of aspen exploded wood lignin." Canadian Journal of Chemistry-Revue Canadienne De Chimie **60**(18): 2372-2382.

Marton, J. (1971). Reactions in Alkaline Pulping. Lignins : Occurrence, Formation, Structure and Reactions. K. V. Sarkanen and C. H. Ludwig. New York, Wiley-Interscience**:** 639-694.

Mathur, R. B., O. P. Bahl, et al. (1988). "Modification of Pan Precursor - Its Influence on the Reaction-Kinetics." Carbon **26**(3): 295-301.

Matsumoto, T. (1985). "Mesophase pitch and its carbon-fibers." Pure and Applied Chemistry **57**(11): 1553-1562.

Messersmith, P. B. and E. P. Giannelis (1995). "Synthesis and Barrier Properties of Poly(Epsilon-Caprolactone)-Layered Silicate Nanocomposites." Journal of Polymer Science Part a-Polymer Chemistry **33**(7): 1047-1057.

Mikawa, S. (1970). "Lignin-based carbon fiber." Chemical Economy & Engineering Review **2**(8): 43-46.

Mochida, I., K. Shimizu, et al. (1990). "Preparation of Mesophase Pitch from Aromatic-Hydrocarbons by the Aid of Hf/Bf3." Carbon **28**(2-3): 311-319.

Mochida, I., K. Shimizu, et al. (1992). "Mesophase Pitch Catalytically Prepared from Anthracene with Hf Bf3." Carbon **30**(1): 55-61.

Mochida, I., Y. Sone, et al. (1985). "Preparation and Properties of Carbonaceous Mesophase .2. Highly Soluble Mesophase from Ethylene Tar Modified Using Aluminum-Chloride as a Catalyst." Carbon **23**(2): 175-178.

Morgan, P. E. (2005). Carbon Fibers and Their Composites. Boca Raton, Taylor & Francis Group.

Nam, P. H., P. Maiti, et al. (2001). "A hierarchical structure and properties of intercalated polypropylene/clay nanocomposites." Polymer **42**(23): 9633-9640.

Nimts, F. G., A. A. Geller, et al. (1986). "Structure features of polyacrylonitrile gel-fibres." Fibre Chemistry **18**(3): 11-13.

Nour, M. A. (2002). "Polymer/clay nanocomposites." Polimery **47**(5): 326-331.

Novak, B. M. (1993). "Hybrid Nanocomposite Materials - between Inorganic Glasses and Organic Polymers." Advanced Materials **5**(6): 422-433.

Oasmaa, A. and E. Kuoppala (2003). "Fast pyrolysis of forestry residue. 3. Storage stability of liquid fuel." Energy & Fuels **17**(4): 1075-1084.

Okada, A. and A. Usuki (1995). "The chemistry of polymer-clay hybrids." Materials Science & Engineering C-Biomimetic Materials Sensors and Systems **3**(2): 109-115.

Otani, S. (1982). Latently anisotropic pitch. Japan, Fuji Standard research Inc.

Otani, S., Y. Fukuoka, et al. (1969). Method for producing carbonized lignin fiber. United States, Nippon Kayaku Co.

Park, Y. D. and I. Mochida (1989). "A 2-Stage Preparation of Mesophase Pitch from the Vacuum Residue of Fcc Decant Oil." Carbon **27**(6): 925-929.

Pavlidou, S. and C. D. Papaspyrides (2008). "A review on polymer-layered silicate nanocomposites." Progress in Polymer Science **33**(12): 1119-1198.

Pickel, J. M., W. L. Griffith, et al. (2006). "Utilization of lignin in the production of low-cost carbon fiber." Abstracts of Papers of the American Chemical Society **231**: 133-CELL.

Pierson, H. O. (1993). Handbook of Carbon, Graphite, Diamond and Fullerenes: Properties, Processing and Applications. Park Ridge, Noyes Publications.

Pinnavaia, T. J. (1983). "Intercalated Clay Catalysts." Science **220**(4595): 365-371.

Pinnavaia, T. J. and G. W. Beall (2000). Polymer-clay nanocomposites. New York, Wiley-Interscience.

Ralph, J., K. Lundquist, et al. (2004). "Lignins: Natural polymers from oxidative coupling of 4-hydroxyphenylpropanoids." Phytochemistry Reviews **3**(1-2): 29-60.

Ralph, J., J. M. Marita, et al. (1999). Solution-State NMR of Lignins. Advances in Lignocellulosics Characterization. D. S. Argyropoulos. Atlanta, TAPPI Press**:** 55-108.

Ralph, S. A., J. Ralph, et al. (2001). NMR database of lignin and cell wall model compounds, http://ars.usda.gov/Services/docs.htm?docid=10491.

Ray, S. S. and M. Okamoto (2003). "Polymer/layered silicate nanocomposites: a review from preparation to processing." Progress in Polymer Science **28**(11): 1539-1641.

Sarkanen, K. V. and C. H. Ludwig (1971). Lignins : Occurrence, Formation, Structure and Reactions. New York, Wiley-Interscience.

Scholze, B., C. Hanser, et al. (2001). "Characterization of the water-insoluble fraction from fast pyrolysis liquids (pyrolytic lignin) Part II. GPC, carbonyl goups, and C-13-NMR." Journal of Analytical and Applied Pyrolysis **58**: 387-400.

Scholze, B. and D. Meier (2001). "Characterization of the water-insoluble fraction from pyrolysis oil (pyrolytic lignin). Part I. PY-GC/MS, FTIR, and functional groups." Journal of Analytical and Applied Pyrolysis **60**(1): 41-54.

Sederoff, R. R. and H. M. Chang (1991). Lignin Biosynthesis. Wood Structure and Composition. M. Lewin and I. S. Goldstein. New York, Marcel Dekker**:** 263-286.

Shen, Z., H. Guo, et al. (1996). Study on Structure and Performance of Graphite Fiber from Mesophase Pitch. Carbon and Carbonaceous Composite Materials: Structure-Property Relationships. K. R. Palmer, D. T. Marx and M. A. Wright. Singapore, World Scientific Publishing**:** 148-154.

Smook, G. A. (1992). Handbook for Pulp and Paper Technologists. Atlanta, TAPPI.

Sonobe, N., T. Kyotani, et al. (1988a). "Formation of highly oriented graphite from poly(acrylonitrile) prepared between the lamellae of montmorillonite." Journal of Physical Chemistry **92**(24): 7029-7034.

Sonobe, N., T. Kyotani, et al. (1988b). "Carbonization of polyacrylonitrile in a two-dimensional space between montmorillonite lamellae." Carbon **26**(4): 573-578.

Sonobe, N., T. Kyotani, et al. (1990). "Carbonization of polyfurfuryl alcohol and polyvinyl acetate between the lamellae of montmorillonite." Carbon **28**(4): 483-488.

Sonobe, N., T. Kyotani, et al. (1991). "Formation of graphite thin-film from polyfurfuryl alcohol and polyvinyl acetate carbons prepared between the lamellae of montmorillonite." Carbon **29**(1): 61-67.

Sperling, L. H. (2005). Introduction to Physical Polymer Science. Hoboken, Wiley-Interscience.

Sudo, K., M. Okoshi, et al. (1988). "Carbon-fiber from lignin--improvement of conversion process of lignin." Abstracts of Papers of the American Chemical Society **195**: 107-CELL.

Sudo, K. and K. Shimizu (1992). "A new carbon-fiber from lignin." Journal of Applied Polymer Science **44**(1): 127-134.

Sudo, K., K. Shimizu, et al. (1993). "A new modification method of exploded lignin for the preparation of a carbon-fiber precursor." Journal of Applied Polymer Science **48**(8): 1485-1491.

Tagawa, T. and T. Miyata (1997). "Size effect on tensile strength of carbon fibers." Materials Science and Engineering a-Structural Materials Properties Microstructure and Processing **238**(2): 336-342.

Tomizuka, I. and D. J. Johnson (1978). "Microvoids in pitch-based and lignin-based carbon fibres as observed by X- ray small angle scattering." Yogyo-Kyokai-Shi **86**(4): 186-192.

Tomizuka, I., T. Kurita, et al. (1971). "Voids in the carbon fibers produced from lignin and PVA." Yogyo-Kyokai-Shi **79**(12): 460-469.

Uraki, Y., S. Kubo, et al. (1995). "Preparation of carbon-fibers from organosolv lignin obtained by aqueous acetic-acid pulping." Holzforschung **49**(4): 343-350.

Usuki, A., Y. Kojima, et al. (1993). "Synthesis of nylon 6-clay hybrid." Journal of Materials Research **8**(5): 1179-1184.

Vaia, R. A., H. Ishii, et al. (1993). "Synthesis and properties of 2-dimensional nanostructures by direct intercalation of polymer melts in layered silicates." Chemistry of Materials **5**(12): 1694-1696.

Walker, J. C. F. (2007). Primary wood processing: principles and practice. Dordrecht, The Netherlands, Springer.

Wang, Z. and T. J. Pinnavaia (1998). "Nanolayer reinforcement of elastomeric polyurethane." Chemistry of Materials **10**(12): 3769-3771.

Yano, K., A. Usuki, et al. (1993). "Synthesis and properties of polyimide clay hybrid." Journal of Polymer Science Part a-Polymer Chemistry **31**(10): 2493-2498.

Zakzeski, J., P. C. A. Bruijnincx, et al. (2010). "The Catalytic valorization of lignin for the production of renewable chemicals." Chemical Reviews **110**(6): 3552-3599.

Zanetti, M., S. Lomakin, et al. (2000). "Polymer layered silicate nanocomposites." Macromolecular Materials and Engineering **279**(6): 1-9.

Zhao, X. B., K. K. Cheng, et al. (2009). "Organosolv pretreatment of lignocellulosic biomass for enzymatic hydrolysis." Applied Microbiology and Biotechnology **82**(5): 815-827.